One plus two-body random matrix ensembles with parity: Density of states and parity ratios

Manan Vyas,[1] V. K. B. Kota,[1,2,*] and P. C. Srivastava[1]
[1]*Physical Research Laboratory, Ahmedabad 380 009, India*
[2]*Department of Physics, Laurentian University, Sudbury, Ontario, Canada P3E 2C6*
(Received 25 January 2011; revised manuscript received 23 March 2011; published 3 June 2011)

One plus two-body embedded Gaussian orthogonal ensemble of random matrices with parity [EGOE(1 + 2)-π] generated by a random two-body interaction (modeled by GOE in two-particle spaces) in the presence of a mean field for spinless identical fermion systems is defined, generalizing the two-body ensemble with parity analyzed by Papenbrock and Weidenmüller [Phys. Rev. C **78**, 054305 (2008)], in terms of two mixing parameters and a gap between the positive ($\pi = +$) and negative ($\pi = -$) parity single-particle (sp) states. Numerical calculations are used to demonstrate, using realistic values of the mixing parameters appropriate for some nuclei, that the EGOE(1 + 2)-π ensemble generates Gaussian form (with corrections) for fixed parity eigenvalue densities (i.e., state densities). The random matrix model also generates many features in parity ratios of state densities that are similar to those predicted by a method based on the Fermi-gas model for nuclei. We have also obtained, by applying the formulation due to Chang *et al.* [Ann. Phys. (NY) **66**, 137 (1971)], a simple formula for the spectral variances defined over fixed-(m_1, m_2) spaces, where m_1 is the number of fermions in the positive parity sp states and m_2 is the number of fermions in the negative parity sp states. Similarly, using the binary correlation approximation, in the dilute limit, we have derived expressions for the lowest two-shape parameters. The smoothed densities generated by the sum of fixed-(m_1, m_2) Gaussians with lowest two-shape corrections describe the numerical results in many situations. The model also generates preponderance of positive parity ground states for small values of the mixing parameters, and this is a feature seen in nuclear shell-model results.

DOI: 10.1103/PhysRevC.83.064301 PACS number(s): 21.60.Cs, 24.60.Lz, 21.10.Hw, 21.10.Ma

I. INTRODUCTION

Random matrix theory (RMT), starting with Wigner and Dyson's Gaussian random ensembles [1,2] introduced to describe neutron resonance data [3,4], has emerged as a powerful statistical approach leading to paradigmatic models describing generic properties of complex systems [5–9]. Developments and applications of RMT in nuclear physics in the last 30 years have been reviewed recently by Weidenmüller and collaborators [10,11]. The Wigner-Dyson classical Gaussian orthogonal (GOE), unitary (GUE), and symplectic (GSE) ensembles are ensembles of multibody interactions, while the nuclear interparticle interactions are essentially two body in nature. This, together with nuclear shell-model examples, led to the introduction of random matrix ensembles generated by two-body interactions in 1970–1971 [12,13]. These two-body ensembles are defined by representing the two-particle Hamiltonian by one of the classical ensembles, and then the m-particle ($m > 2$) H matrix is generated by the Hilbert space geometry. Thus, the random matrix ensemble in the two-particle spaces is embedded in the m-particle H matrix and, therefore, these ensembles are generically called embedded ensembles (EEs). The simplest of these ensembles is the embedded Gaussian orthogonal ensemble of random matrices generated by two-body interactions for spinless fermion (boson) systems, denoted by EGOE(2) [BEGOE(2); here, B stands for bosons]. In addition to the complexity generating two-body interaction, Hamiltonians for realistic systems such as nuclei consist of a mean-field one-body part. Then, the appropriate random matrix ensembles are EE(1 + 2). The spinless fermion and boson EGEs (orthogonal and unitary versions) have been explored in detail from the 1970s with a major revival from 1995, and it is now well understood that EGEs model many-body chaos or stochasticity exhibited by isolated finite interacting quantum systems [9,14]. Aside from the mean field and the two-body character, realistic Hamiltonians also carry a variety of symmetries. In many applications of EGEs, generic properties of EGEs for spinless fermions are "assumed" to extend to symmetry subspaces [15]. More importantly, there are several properties of real systems that require explicit inclusion of symmetries, and they are defined by a variety of Lie algebras. This led to studies on EGEs with symmetries such as spin [16–20], spin-isospin SU(4) [21], J symmetry [22], and many others (see, for example, [23,24]). In this paper, we consider parity symmetry in EE as there are several nuclear structure quantities that require explicit inclusion of parity. Some of these are as follows.

Parity ratios of nuclear level densities are an important ingredient in nuclear astrophysical applications. Recently, a method based on the noninteracting Fermi-gas model for proton-neutron systems has been developed, and the parity (π) ratios as a function of excitation energy in a large number of nuclei of astrophysical interest have been tabulated [25]. The method is based on the assumption that the probability to occupy s out of N given single-particle (sp) states follows Poisson distribution in the dilute limit ($m \ll N, N \to \infty$, where m is the number of particles). Then, the ratio of the partition functions for the positive ($+ve$) and negative ($-ve$) parity states is given by the simple formula $Z_-/Z_+ = \tanh f$, where f is average number of particles in the $+ve$ parity states. Starting with this, an iterative method is developed

*vkbkota@prl.res.in

with inputs from the Fermi-Dirac distribution for occupancies including pairing effects and the Fermi-gas form for the total level density. In the examples studied in [25], parity ratios are found to equilibrate only around 5–10 MeV excitation energy. However, *ab initio* interacting particle theory for parity ratios is not yet available.

A closely related question is about the form of the density of states defined over spaces with fixed π. In general, fixed-π density of states can be written as a sum of appropriate partial densities. In the situation wherein the form of the partial densities is determined by a few parameters (as it is with a Gaussian or a Gaussian with one or two corrections), it is possible to derive a theory for these parameters and, by using these, one can construct fixed-π density of states and calculate parity ratios. Such a theory with interactions, in general, follows from random matrix theory [15].

In addition to the questions related to fixed-π density of states and parity ratios, there is also the important recognition in the past few years that random interactions generate regular structures [22,26,27]. It was shown in [28] that the shell model for even-even nuclei gives preponderance of $+ve$ parity ground states. A parameter-free EGOE with parity has been defined and analyzed recently [29] to address the question of preponderance of ground states with positive parity for systems with even number of fermions. They show that, in the dilute limit, $+ve$ parity ground states appear with only 50% probability. Thus, a random matrix theory describing shell-model results is not yet available.

With the success of the embedded random matrix ensembles (EE) [9,14], one can argue that the EE generated by parity preserving random interaction may provide generic results for the three nuclear structure quantities mentioned above. For nuclei, the GOE versions of EE are relevant. Then, with a random (modeled by GOE) two-body interaction preserving parity in the presence of a mean field, we have embedded Gaussian orthogonal ensemble of one plus two-body interactions with parity [hereafter called EGOE(1 + 2)-π]. This model contains two mixing parameters and a gap between the $+ve$ and $-ve$ parity sp states and it goes much beyond the simpler model considered in [29]. In the random matrix model used in this paper, proton-neutron degrees of freedom and angular momentum (J) are not considered. Let us add that, in this paper, for the first time, a random matrix theory for parity ratios is attempted. Now we will give a preview.

Section II gives the definition of EGOE(1 + 2)-π and a method for its construction. From the results known for EE for spinless fermion (boson) systems, for fermions (bosons) with spin and from shell-model calculations [3,14,18], it is expected that the fixed-π state densities (more appropriately partial densities) approach Gaussian form in general. Therefore, exact propagation formulas for fixed-π energy centroids and spectral variances are derived and the results are given in Sec. III. Used here is the group theoretical formulation developed by Chang *et al.* [30]. Similarly, in Appendix B, the formulas are given for the ensemble averaged skewness $\gamma_1(m_1, m_2)$ and excess $\gamma_2(m_1, m_2)$ parameters for fixed-(m_1, m_2) partial densities (with m_1 fermions distributed in N_+ number of $+ve$ parity sp levels and, similarly, m_2 fermions in N_- number of $-ve$ parity sp levels) and used is the binary correlation approximation method described in [31–34]. These will provide corrections to the Gaussian state densities. In Sec. IV, we present the numerical results for (i) fixed-π state densities, (ii) parity ratios of state densities, and (iii) probability for $+ve$ parity ground states. Finally, Sec. V gives conclusions and future outlook.

II. EGOE(1 + 2)-π ENSEMBLE

Given N_+ number of positive parity sp states and, similarly, N_- number of negative parity sp states, let us assume, for simplicity, that the $+ve$ and $-ve$ parity states are degenerate and separated by energy Δ (see Fig. 1). This defines the one-body part $h(1)$ of the Hamiltonian H with $N = N_+ + N_-$ sp states. The matrix for the two-body part $V(2)$ of H [we assume H is (1 + 2)-body] will be a 3×3 block matrix in two-particle spaces as there are three possible ways to generate two-particle states with definite parity: (i) both fermions in $+ve$ parity states, (ii) both fermions in $-ve$ parity states, and (iii) one fermion in $+ve$ and the other fermion in $-ve$ parity states. They will give the matrices A, B, and C, respectively, in Fig. 1. For parity preserving interactions, only the states (i) and (ii) will be mixed, and the mixing matrix is D in Fig. 1. Note that the matrices A, B, and C are symmetric square matrices, while D is in general a rectangular mixing matrix. Consider N sp states arranged such that the states 1 to N_+ have $+ve$ parity and states $N_+ + 1$ to N have $-ve$ parity. Then, the operator form of H preserving parity is

$$
\begin{aligned}
H &= h(1) + V(2), \\
h(1) &= \sum_{i=1}^{N_+} \epsilon_i^{(+)} \hat{n}_i^{(+)} + \sum_{i=N_++1}^{N} \epsilon_i^{(-)} \hat{n}_i^{(-)}, \\
\epsilon_i^{(+)} &= 0, \quad \epsilon_i^{(-)} = \Delta, \\
V(2) &= \sum_{\substack{i,j,k,l=1 \\ (i<j,\,k<\ell)}}^{N_+} \langle \nu_k \nu_\ell | V | \nu_i \nu_j \rangle a_k^\dagger a_\ell^\dagger a_j a_i \\
&\quad + \sum_{\substack{i',j',k',\ell'=N_++1 \\ (i'<j',\,k'<\ell')}}^{N} \langle \nu_{k'} \nu_{\ell'} | V | \nu_{i'} \nu_{j'} \rangle a_{k'}^\dagger a_{\ell'}^\dagger a_{j'} a_{i'} \\
&\quad + \sum_{i'',k''=1}^{N_+} \sum_{j'',\ell''=N_++1}^{N} \langle \nu_{k''} \nu_{\ell''} | V | \nu_{i''} \nu_{j''} \rangle a_{k''}^\dagger a_{\ell''}^\dagger a_{j''} a_{i''} \\
&\quad + \sum_{\substack{P,Q=1 \\ (P<Q)}}^{N_+} \sum_{\substack{R,S=N_++1 \\ (R<S)}}^{N} \\
&\quad \times [\langle \nu_P \nu_Q | V | \nu_R \nu_S \rangle a_P^\dagger a_Q^\dagger a_S a_R + \text{h.c.}].
\end{aligned}
\tag{1}
$$

In Eq. (1), the ν_i's are sp states with $i = 1, 2, \ldots, N$ (the first N_+ states are $+ve$ parity and the remaining states are $-ve$ parity). Similarly, $\langle \cdots | V | \cdots \rangle$ are the two-particle matrix elements, $\hat{n}_i$ are number operators, and $a_i^\dagger$ and a_i are creation and annihilation operators, respectively. Note that the four terms in the right-hand side of the expression for $V(2)$ in

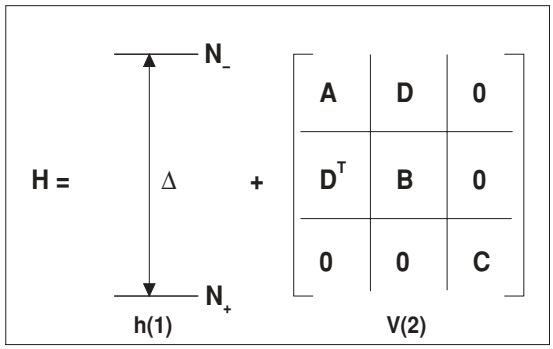

FIG. 1. Parity preserving one plus two-body H with a sp spectrum defining $h(1)$ along with a schematic form of the $V(2)$ matrix. Dimension of the matrices A, B, and C are $N_+(N_+ - 1)/2$, $N_-(N_- - 1)/2$, and N_+N_-, respectively. Note that D^T is the transpose of the matrix D. See text for details.

Eq. (1) correspond, respectively, to the matrices A, B, C, and D shown in Fig. 1.

Many-particle states for m fermions in the N sp states can be obtained by distributing m_1 fermions in the $+ve$ parity sp states (N_+ in number) and, similarly, m_2 fermions in the $-ve$ parity sp states (N_- in number) with $m = m_1 + m_2$. Let us denote each distribution of m_1 fermions in N_+ sp states by $\mathbf{m}_1$ and, similarly, $\mathbf{m}_2$ for m_2 fermions in N_- sp states. The many-particle basis defined by $(\mathbf{m}_1, \mathbf{m}_2)$ with m_2 even will form the basis for $+ve$ parity states and, similarly, with m_2 odd for $-ve$ parity states. In the $(\mathbf{m}_1, \mathbf{m}_2)$ basis with m_2 even (or odd), the H matrix construction reduces to the matrix construction for spinless fermion systems. The method of construction for spinless fermion systems is well known [14] and, therefore, it is easy to construct the many-particle H matrices in $+ve$ and $-ve$ parity spaces. The matrix dimensions d_+ for $+ve$ parity and d_- for $-ve$ parity spaces are given by

$$d_+ = \sum_{m_1,m_2(m_2\ \text{even})} \binom{N_+}{m_1}\binom{N_-}{m_2},$$
$$d_- = \sum_{m_1,m_2(m_2\ \text{odd})} \binom{N_+}{m_1}\binom{N_-}{m_2}. \tag{2}$$

Some examples for the dimensions d_+ and d_- are given in Table I.

The EGOE$(1+2)$-π ensemble is defined by choosing the matrices A, B, and C to be independent GOEs with matrix elements variances v_a^2, v_b^2, and v_c^2, respectively. Similarly, the matrix elements of the mixing D matrix are chosen to be independent (independent of A, B, and C matrix elements) zero-centered Gaussian variables with variance v_d^2. Without loss of generality, we choose $\Delta = 1$ so that all the v's are in Δ units. This general EGOE$(1+2)$-π model will have too many parameters $(v_a^2, v_b^2, v_c^2, v_d^2, N_+, N_-, m)$ and, therefore, it is necessary to reduce the number of parameters. A numerically tractable and physically relevant (as discussed below) restriction is to choose the matrix element variances of the diagonal blocks A, B, and C to be the same, and then we have the EGOE$(1+2)$-π model defined by (N_+, N_-, m) and the variance parameters (τ,α), where

$$\frac{v_a^2}{\Delta^2} = \frac{v_b^2}{\Delta^2} = \frac{v_c^2}{\Delta^2} = \tau^2, \quad \frac{v_d^2}{\Delta^2} = \alpha^2. \tag{3}$$

Thus EGOE$(1+2)$-π we employ is

$$A : \text{GOE}(0 : \tau^2), \quad B : \text{GOE}(0 : \tau^2),$$
$$C : \text{GOE}(0 : \tau^2), \quad D : \text{GOE}(0 : \alpha^2), \tag{4}$$
$$A, B, C, D \text{ are independent GOEs.}$$

Note that the D matrix is a GOE only in the sense that the matrix elements D_{ij} are all independent zero-centered Gaussian variables with variance α^2. In the limit $\tau^2 \to \infty$ and $\alpha = \tau$, the model defined by Eqs. (1), (3), and (4) reduces to the simpler model analyzed in [29].

Before proceeding further, it is useful to mention that we are considering in this paper spinless fermion systems (with parity included) just as in the previous investigation [29]. It is possible to extend the ensemble to nucleons in shell-model j orbits (including both $+ve$ and $-ve$ orbits such as, for example, sd and fp) and construct the ensemble in many-nucleon spaces with a given J^π or $J^\pi T$ using a shell-model code. However, such an attempt has not been made, just as in [29], as our focus is on parity. Also, the ensemble for spinless systems will give the essential features due to parity and these can be used in later explorations using ensembles with J^π or $J^\pi T$, which are more complicated numerically and more importantly from an analytical point of view [3,22]. In fact, due to the severe problems associated with analytical tractability, a variety of EGOE are being analyzed since 1995 (see [9,14,22] for reviews). At this point, it is also useful to mention that EGOE$(1+2)$'s are also called TBRE in literature (see Sec. 5.7 in [9] for clarifications on this nomenclature). Brody *et al.* state the following [3]: "*The most severe mathematical difficulties with TBRE are due to angular momentum constraints . . .. Another type of ensemble, . . . much closer to being mathematical tractable abandons the J restrictions entirely . . . an embedded GOE, or EGOE for short.*"

Starting with the EGOE$(1+2)$-π ensemble defined by Eqs. (1), (3), and (4), we have numerically constructed

TABLE I. Hamiltonian matrix dimensions d_+ and d_- for various values of (N_+, N_-, m).

N_+	N_-	m	d_+	d_-	N_+	N_-	m	d_+	d_-
6	6	6	452	472	8	8	4	924	896
7	5	6	462	462			5	2184	2184
7	7	5	1001	1001			6	3976	4032
		6	1484	1519	10	6	4	900	920
		7	1716	1716			5	2202	2166
8	6	5	1016	986			6	4036	3972
		6	1499	1504	6	10	4	900	920
9	5	5	1011	911			5	2166	2202
		6	1524	1479			6	4036	3972
5	10	4	665	700	9	9	6	9240	9324
		5	1501	1502	10	8	6	9268	9296
					10	10	5	7752	7752
							6	19 320	19 440

100 (in some examples 200) members of the ensemble in many-particle $+ve$ and $-ve$ parity spaces with dimensions d_+ and d_- given by Eq. (2) for several values of (N_+, N_-, m) and varying the parameters τ and α. This means that we have considered 100 realizations of EGOE(1 + 2)-π random matrices in (N_+, N_-, m) spaces; we use the phrase "members" throughout the paper instead of "realizations" (other names used by some authors are "sets," "samples," and "trials") as in all our previous papers. Before discussing the numerical calculations, we present the results for the energy centroids, variances, and also the shape parameters (skewness and excess) defining the normalized fixed-(m_1, m_2) partial densities

$$\rho^{m_1,m_2}(E) = \langle \delta(H - E) \rangle^{m_1,m_2} = \frac{1}{d(m_1, m_2)} \sum_{\alpha,\beta} \left| C^{m_1,m_2,\alpha}_{E,\beta} \right|^2;$$
$$|m_1, m_2, \alpha\rangle = \sum_{\beta} C^{m_1,m_2,\alpha}_{E,\beta} \, |E, \beta\rangle \, , \tag{5}$$

where, $\langle \cdots \rangle$ corresponds to average and α and β are extra labels required to specify completely the states with a given (m_1, m_2) and E, respectively. Later, we use the symbol $\langle\langle \cdots \rangle\rangle$ that denotes the trace. These will allow us to understand some of the numerical results. Let us add that the fixed-π eigenvalue densities $I_\pm(E)$ are sums of the appropriate partial densities as given by Eq. (16) below. Note that the densities $I_\pm(E)$ are normalized to $d_\pm$.

III. ENERGY CENTROIDS, VARIANCES, SKEWNESS, AND EXCESS PARAMETERS FOR FIXED-(m_1, m_2) PARTIAL DENSITIES

Let us call the set of $+ve$ parity sp states as unitary orbit no. 1 and, similarly, the set of $-ve$ parity sp states as unitary orbit no. 2; see [15] for unitary orbits notation and significance. For convenience, from now on, we denote the sp states by the letters $(i, j, \ldots)$ and unitary orbits by Greek letters $(\alpha, \beta, \ldots)$. Note that $\alpha = 1$ corresponds to the $+ve$ parity unitary orbit and $\alpha = 2$ corresponds to the $-ve$ parity unitary orbit (with this notation, $N_1 = N_+$ and $N_2 = N_-$). The sp states that belong to a unitary orbit α are denoted as $i_\alpha, j_\alpha, \ldots$. Propagation formulas for the energy centroids and variances of the partial densities $\rho^{m_1,m_2}(E)$ follow from the unitary decomposition of $V(2)$ with respect to the subalgebra $U(N_+) \oplus U(N_-)$ contained in $U(N)$. Note that (m_1, m_2) label the irreducible representations (irreps) of $U(N_+) \oplus U(N_-)$ and they all belong to the $U(N)$ irreps labeled by m. The (m_1, m_2) are often called unitary configurations [15]. With respect to $U(N_+) \oplus U(N_-)$, the operator $V(2)$ decomposes into three parts $V(2) \to V^{[0]} + V^{[1]} + V^{[2]}$. The $V^{[0]}$ generates the energy centroids $\langle V \rangle^{m_1,m_2}$, $V^{[1]}$ corresponds to the algebraic mean field generated by V, and $V^{[2]}$ is the remaining irreducible two-body part. By extending the unitary decomposition for the situation with a single orbit for spinless fermions (given in Appendix A) and also using the detailed results in [30], we obtain the following formulas for the $V^{[\nu]}$'s.

The $V^{[0]}$ is given by (with $\alpha = 1, 2$ and $\beta = 1, 2$)

$$V^{[0]} = \sum_{\alpha \geqslant \beta} \frac{\hat{n}_\alpha(\hat{n}_\beta - \delta_{\alpha\beta})}{(1 + \delta_{\alpha\beta})} V_{\alpha\beta},$$
$$V_{\alpha\alpha} = \binom{N_\alpha}{2}^{-1} \sum_{i>j} V_{i_\alpha j_\alpha i_\alpha j_\alpha}, \tag{6}$$
$$V_{\alpha\beta} = (N_\alpha N_\beta)^{-1} \sum_{i,j} V_{i_\alpha j_\beta i_\alpha j_\beta}; \quad \alpha \neq \beta.$$

Then, the traceless part $\widetilde{V} = V - V^{[0]} = V^{[1]} + V^{[2]}$, where $(\widetilde{V})_{i_\alpha j_\beta i_\alpha j_\beta} = V_{i_\alpha j_\beta i_\alpha j_\beta} - V_{\alpha\beta}$ and $(\widetilde{V})_{ijk\ell} = V_{ijk\ell}$ for all others. Now, the $V^{[1]}$ part is

$$V^{[1]} = \sum_{i_\alpha, j_\alpha} \widehat{\xi}_{i_\alpha j_\alpha} a^\dagger_{i_\alpha} a_{j_\alpha},$$
$$\widehat{\xi}_{i_\alpha j_\alpha} = \sum_{\beta} \frac{\hat{n}_\beta - \delta_{\alpha\beta}}{N_\beta - 2\delta_{\alpha\beta}} \zeta_{i_\alpha j_\alpha}(\beta), \tag{7}$$
$$\zeta_{i_\alpha j_\alpha}(\beta) = \sum_{k_\beta} \widetilde{V}_{k_\beta i_\alpha k_\beta j_\alpha}.$$

Finally, the $V^{[2]}$ part is as follows:

$$V^{[2]} = \widetilde{V} - V^{[1]},$$
$$V^{[2]}_{i_\alpha j_\beta i_\alpha j_\beta} = \widetilde{V}_{i_\alpha j_\beta i_\alpha j_\beta} - \left[\frac{\zeta_{i_\alpha j_\alpha}(\beta)}{N_\beta - 2\delta_{\alpha\beta}} + \frac{\zeta_{i_\beta j_\beta}(\alpha)}{N_\alpha - 2\delta_{\alpha\beta}} \right],$$
$$V^{[2]}_{k_\alpha i_\beta k_\alpha j_\beta} = \widetilde{V}_{k_\alpha i_\beta k_\alpha j_\beta} - \frac{\zeta_{i_\beta j_\beta}(\alpha)}{N_\alpha - 2\delta_{\alpha\beta}}; \quad i_\beta \neq j_\beta, \tag{8}$$
$$V^{[2]}_{ijk\ell} = \widetilde{V}_{ijk\ell} \text{ for all others.}$$

Given Eqs. (6), (7), and (8), by intuition and using Eq. (A3), it is possible to write the propagation formulas for the energy centroids and variances of $\rho^{m_1,m_2}(E)$. Note that these are essentially traces of H and H^2 over the space defined by the two-orbit configurations (m_1, m_2) [see Eqs. (9) and (10) below]. A direct approach to write the propagation formulas for centroids and variances for a multiorbit configuration was given in detail first by French and Ratcliff [35]. The formula for the variance given in [35] is cumbersome and it is realized later [30] that they can be made compact by applying group theory (see, also, [14,15,36]). We have adopted the group theoretical approach for the two-orbit averages and obtained formulas. Propagation formula for the fixed-(m_1, m_2) energy centroids is

$$E_c(m_1, m_2) = \langle H \rangle^{m_1,m_2} = m_2 \Delta + \sum_{\alpha \geqslant \beta} \frac{m_\alpha(m_\beta - \delta_{\alpha\beta})}{(1 + \delta_{\alpha\beta})} V_{\alpha\beta}. \tag{9}$$

The first term in Eq. (9) is generated by $h(1)$ and it is simple because of the choice of the sp energies as shown in Fig. 1.

The propagation formula for fixed-(m_1, m_2) variances is

$$\sigma^2(m_1,m_2) = \langle H^2\rangle^{m_1,m_2} - [\langle H\rangle^{m_1,m_2}]^2$$
$$= \sum_\alpha \frac{m_\alpha(N_\alpha - m_\alpha)}{N_\alpha(N_\alpha-1)} \sum_{i_\alpha,j_\alpha} [\xi_{i_\alpha,j_\alpha}(m_1,m_2)]^2 + {\sum_{\alpha,\beta,\gamma,\delta}}' \frac{m_\alpha(m_\beta-\delta_{\alpha\beta})(N_\gamma-m_\gamma)(N_\delta-m_\delta-\delta_{\gamma\delta})}{N_\alpha(N_\beta-\delta_{\alpha\beta})(N_\gamma-\delta_{\gamma\alpha}-\delta_{\gamma\beta})(N_\delta-\delta_{\delta\alpha}-\delta_{\delta\beta}-\delta_{\delta\gamma})}(X),$$
$$\xi_{i_\alpha,j_\alpha}(m_1,m_2) = \sum_\beta \frac{m_\beta-\delta_{\alpha\beta}}{N_\beta-2\delta_{\alpha\beta}} \zeta_{i_\alpha j_\alpha}(\beta), \quad X = {\sum}' \left(V^{[2]}_{i_\alpha j_\beta k_\gamma \ell_\delta}\right)^2. \tag{10}$$

The prime over summations in Eq. (10) implies that the summations are not free sums. Note that $(\alpha, \beta, \gamma, \delta)$ take values (1, 1, 1, 1), (2, 2, 2, 2), (1, 2, 1, 2), (1, 1, 2, 2), and (2, 2, 1, 1). Similarly, in the sum over (i_α, j_β), $i \leqslant j$ if $\alpha = \beta$ and, otherwise, the sum is over all i and j; similarly, for (k_γ, ℓ_δ). Using $E_c(m_1, m_2)$ and $\sigma^2(m_1, m_2)$, the fixed parity energy centroids and spectral variances [they define $I_\pm(E)$] can be obtained as follows:

$$E_c(m,\pm) = \langle H\rangle^{m,\pm} = \frac{1}{d_\pm} {\sum_{m_1,m_2}}' d(m_1,m_2) E_c(m_1,m_2),$$
$$\sigma^2(m,\pm) = \langle H^2\rangle^{m,\pm} - [\langle H\rangle^{m,\pm}]^2, \tag{11}$$
$$\langle H^2\rangle^{m,\pm} = \frac{1}{d_\pm} {\sum_{m_1,m_2}}' d(m_1,m_2)\left[\sigma^2(m_1,m_2) + E_c^2(m_1,m_2)\right].$$

The prime over summations in Eq. (11) implies that m_2 is even (odd) for $+ve$ $(-ve)$ parity.

It should be pointed out that the formulas given by Eqs. (9), (10), and (11) are compact and easy to understand compared to Eqs. (10)–(14) of [29] and also those that follow from Eqs. (129) and (133) of [35], where unitary decomposition is not employed. We have verified Eqs. (9) and (10) by explicit construction of the H matrices in many examples. In principle, it is possible to obtain a formula for the ensemble-averaged variances using Eq. (10); the ensemble-averaged centroids derive only from $h(1)$. Simple asymptotic formulas for ensemble-averaged variances follow by neglecting the δ functions that appear in Eq. (10) and replacing $(V^{[2]}_{ijk\ell})^2$ by τ^2 and α^2 appropriately. Then, the final formula for the ensemble-averaged fixed-(m_1, m_2) variances is

$$\overline{\sigma^2(m_1,m_2)} \approx m\left[\sum_{\alpha=1}^{2} m_\alpha\,(N_\alpha - m_\alpha)\right]\tau^2 + \left[\binom{m_1}{2}\binom{\widetilde{m}_1}{2} + \binom{m_2}{2}\binom{\widetilde{m}_2}{2} + m_1 m_2 \widetilde{m}_1 \widetilde{m}_2\right]\tau^2 + \left[\binom{m_1}{2}\binom{\widetilde{m}_2}{2} + \binom{m_2}{2}\binom{\widetilde{m}_1}{2}\right]\alpha^2. \tag{12}$$

Here, $\widetilde{m}_1 = N_1 - m_1$ and $\widetilde{m}_2 = N_2 - m_2$. The overbar in Eq. (12) denotes ensemble average. In Table II, we compare the results obtained from Eq. (12) with those obtained for various 100-member ensembles using Eq. (10), and the agreements are quite good. Therefore, in many practical applications, one can use Eq. (12).

The skewness and excess parameters γ_1 and γ_2 give information about the shape of the partial densities and they are close to zero implies Gaussian form. Formulas for the M_r, $r = 3, 4$, for a given one plus two-body Hamiltonian defined by Eq. (1) follow from the results given in [36–41] many years back. However, these formulas contain a very large number of complicated terms (in particular, for M_4), and carrying out analytically ensemble averaging has proved to be impractical (we are not aware if anyone was successful in the past). Some idea of the difficulty in carrying out simplifications can be seen from the attempt in [42]. An alternative is to program the exact formulas and evaluate the moments numerically for each member of EGOE$(1 + 2)$-π by considering, say, 500 members in two-particle spaces. As pointed out by Terán and Johnson [43] in their most recent attempt, these calculations for the fourth moments are time consuming if not impractical. All the problems with the exact formulas have been emphasized in [15]. Because of these (in the future with much faster computers, it may be possible to use the exact formulas), we have adopted the binary correlation approximation, first used by Mon and French [31,32] and later by French *et al.* [33,34], which is good in the dilute limit: $m_1, N_1, m_2, N_2 \to \infty$, $m/N_1 \to 0$, and $m/N_2 \to 0$, where m is m_1 or m_2, for deriving formulas for the ensemble averaged M_3 and M_4. The final formulas are given in Appendix B and details of the derivations will be reported elsewhere [44]. The following results are inferred from the results in Appendix B.

It is seen from Eq. (B9) that $\gamma_1(m_1, m_2)$ will be nonzero only when $\alpha \neq 0$ and the τ dependence is weak. Also, it is seen that, for $N_+ = N_-$, $\gamma_1(m_1, m_2) = -\gamma_1(m_2, m_1)$. Similarly, Eq. (B10) shows that, for $N_+ = N_-$, $\gamma_2(m_1, m_2) = \gamma_2(m_2, m_1)$. In the dilute limit, with some approximations as discussed after Eq. (B10), the expression for $\gamma_2(m_1, m_2)$ is given by Eq. (B11). This shows that, for $\alpha \ll \tau$ or $\tau \ll \alpha$, the C_1 and C_2 in Eq. (B11) will be negligible and then $\gamma_2 \sim -4/m$ for $m_1 = m_2 = m/2$ and $N_1 = N_2 = N$. This is same as the result for spinless fermion EGOE(2) [31,32] and shows that, for a range of (τ, α) values, $\rho^{m_1,m_2}(E)$ will be close to Gaussian. Moreover, to the extent that Eq. (B11) applies, the density $\rho^{m_1,m_2}(E)$ is a convolution of the densities generated by $X(2)$ and $D(2)$ operators. Let us add that the binary correlation results presented in Appendix B, with further extensions, will be useful in the study of partitioned EGOE discussed in [14,45].

IV. RESULTS AND DISCUSSION

In order to proceed with the numerical calculations, we need to have some idea of the range of the parameters $(\tau, \alpha, m/N_+, N_+/N_-)$. Toward this end, we have used realistic

TABLE II. Ensemble-averaged fixed-(m_1, m_2) widths $\sigma(m_1, m_2)$ and the total spectral width σ_t for different (τ, α) values. For each (τ, α), the $\sigma(m_1, m_2)$ are given in the table and they are obtained using the exact propagation formula given in Eq. (10) for each member of the ensemble. In all the calculations, ensembles with 100 members are employed. Numbers in the parentheses are obtained by using the asymptotic formula given in Eq. (12). The last row for each (N_+, N_-) gives the corresponding σ_t values. All the results are given for six particle systems and the dimensions $d(m_1, m_2)$ are also given in the table. See text for details.

(N_+, N_-)	m_1	m_2	$d(m_1, m_2)$	$(\tau, \alpha/\tau)$			
				(0.1,0.5)	(0.1,1.5)	(0.2,0.5)	(0.2,1.5)
(8,8)	0	6	28	1.36(1.39)	3.21(3.21)	2.73(2.77)	6.41(6.42)
	1	5	448	1.76(1.79)	2.70(2.72)	3.52(3.57)	5.41(5.44)
	2	4	1960	2.05(2.09)	2.48(2.50)	4.11(4.17)	4.96(5.01)
	3	3	3136	2.16(2.19)	2.42(2.45)	4.31(4.38)	4.84(4.90)
	4	2	1960	2.05(2.09)	2.48(2.50)	4.11(4.17)	4.95(5.01)
	5	1	448	1.76(1.79)	2.70(2.72)	3.52(3.57)	5.41(5.44)
	6	0	28	1.37(1.39)	3.21(3.21)	2.75(2.77)	6.42(6.42)
				2.29(2.32)	2.68(2.71)	4.24(4.30)	5.08(5.13)
(6,10)	0	6	210	1.67(1.70)	2.70(2.72)	3.34(3.41)	5.41(5.44)
	1	5	1512	2.04(2.07)	2.48(2.51)	4.08(4.15)	4.97(5.02)
	2	4	3150	2.19(2.22)	2.41(2.44)	4.37(4.44)	4.82(4.88)
	3	3	2400	2.11(2.14)	2.43(2.46)	4.22(4.28)	4.86(4.91)
	4	2	675	1.84(1.87)	2.60(2.62)	3.67(3.73)	5.20(5.24)
	5	1	60	1.46(1.48)	3.06(3.06)	2.92(2.96)	6.12(6.13)
	6	0	1	1.30(1.30)	3.90(3.90)	2.60(2.60)	7.81(7.79)
				2.31(2.33)	2.65(2.67)	4.30(4.36)	5.02(5.07)
(10,10)	0	6	210	1.97(2.01)	4.16(4.19)	3.95(4.01)	8.33(8.37)
	1	5	2520	2.44(2.49)	3.63(3.66)	4.90(4.98)	7.25(7.32)
	2	4	9450	2.76(2.81)	3.36(3.40)	5.53(5.61)	6.71(6.79)
	3	3	14400	2.87(2.92)	3.28(3.32)	5.74(5.83)	6.56(6.64)
	4	2	9450	2.76(2.81)	3.36(3.40)	5.53(5.61)	6.71(6.79)
	5	1	2520	2.44(2.49)	3.63(3.66)	4.90(4.98)	7.25(7.32)
	6	0	210	1.97(2.01)	4.16(4.19)	3.95(4.01)	8.33(8.37)
				2.95(2.99)	3.54(3.57)	5.62(5.70)	6.83(6.91)

nuclear effective interactions in $sdfp$ [46] and $fpg_{9/2}$ [47] spaces and calculated the variances v_a^2, v_b^2, v_c^2, v_d^2 for these interactions. Note that it is easy to identify the matrices A, B, C, and D given the interaction matrix elements $\langle (j_1 j_2) JT|V|(j_3 j_4) JT\rangle$. To calculate the mean-squared matrix elements v^2's, we set the diagonal two-particle matrix elements to zero and use the weight factor $(2J+1)(2T+1)$. By assuming that $\Delta = 3$ and 5 MeV (these are reasonable values for $A = 20-80$ nuclei), we obtain $\tau \sim 0.09-0.24$ and $\alpha \sim (0.9–1.3) \times \tau$. These deduced values of α and τ clearly point out that one has to go beyond the highly restricted ensemble employed in [29] and it is necessary to consider the more general EGOE$(1+2)$-π defined in Sec. II. Similarly, for $sdfp$ and $fpg_{9/2}$ spaces, $N_+/N_- \sim 0.5-2.0$. Finally, for nuclei with m number of valence nucleons (particles or holes), where $sdfp$ or $fpg_{9/2}$ spaces are appropriate, usually $m \lesssim N_+$ or N_-, whichever is lower. Given these, we have selected the following examples: $(N_+, N_-, m) = (8, 8, 4)$, $(8, 8, 5)$, $(10, 6, 4)$, $(10, 6, 5)$, $(6, 10, 4)$, $(6, 10, 5)$, $(8, 8, 6)$, $(6, 6, 6)$, $(7, 7, 7)$, and $(7, 7, 6)$. To go beyond the matrix dimensions $\sim$5000 with 100 members is not feasible at present with the High Performance Computing (HPC) cluster that is used for all the calculations. Most of the discussion in this paper is restricted to $N = N_+ + N_- = 16$ and $m \ll N$ as in this dilute limit, it is possible to understand the ensemble results better. Following the nuclear examples mentioned above, we have chosen $\tau = 0.05, 0.1, 0.2, 0.3$ and $\alpha/\tau = 0.5, 1.0, 1.5$. We will make some comments on the results for other (τ, α) values at appropriate places.

Now we will present the results for (i) the form of the $+ve$ and $-ve$ parity state densities $I_+(E)$ and $I_-(E)$, respectively, (ii) the parity ratios $I_-(E)/I_+(E)$ versus E, where E is the excitation energy of the system, and (iii) the probability for $+ve$ parity ground states generated by the EGOE$(1+2)$-π ensemble.

A. Gaussian form for fixed-π state densities

By using the method discussed in Sec. II, we have numerically constructed in $+ve$ and $-ve$ parity spaces EGOE$(1+2)$-π ensembles of random matrices consisting of 100 Hamiltonian matrices in large number of examples, i.e., for (N_+, N_-, m) and (τ, α) parameters mentioned above. By diagonalizing these matrices, ensemble-averaged eigenvalue (state) densities

$$\overline{I_\pm(E)} = \overline{\langle\langle \delta(H-E)\rangle\rangle^\pm} \tag{13}$$

are constructed. From now on, we drop the overbar symbol when there is no confusion. Results are shown for $(N_+, N_-, m) = (8, 8, 4)$, $(8, 8, 5)$, $(10, 6, 5)$, and $(6, 10, 5)$ for

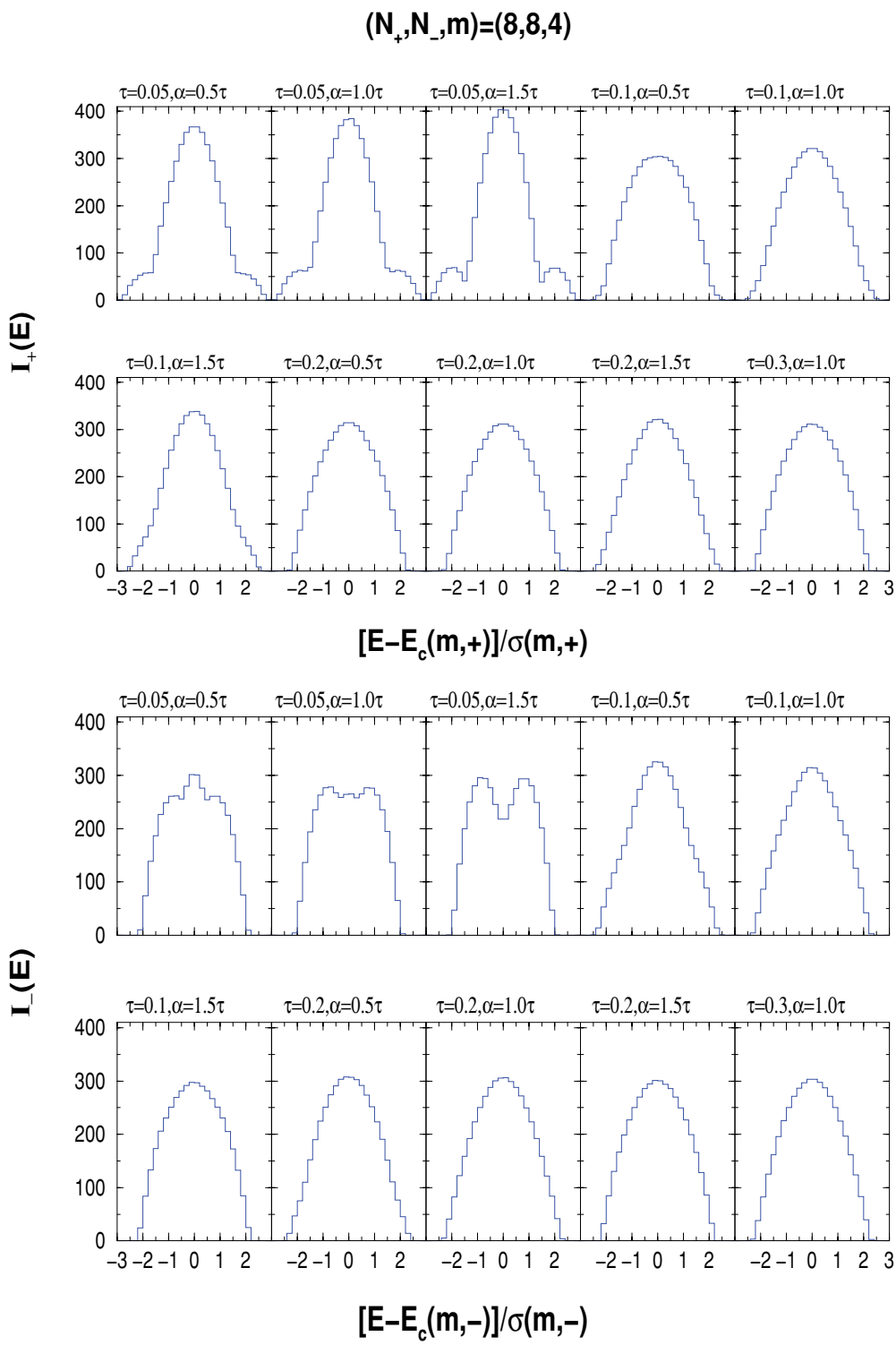

FIG. 2. (Color online) Positive and negative parity state densities for various (τ, α) values for $(N_+, N_-, m) = (8, 8, 4)$ system. See text for details.

several values of (τ, α) in Figs. 2, 3, and 4. To construct the fixed-parity eigenvalue densities, we first make the centroids $E_c(m, \pm)$ of all the members of the ensemble to be zero and variances $\sigma^2(m, \pm)$ to be unity, i.e. for each member we have the standardized eigenvalues $\widehat{E} = [E - E_c(m, \pm)]/\sigma(m, \pm)$. Then, by combining all the $\widehat{E}$ and using a bin size $\Delta\widehat{E} = 0.2$, histograms for $I_\pm(E)$ are generated. It is seen that the state densities are multimodal for small τ values and, for $\tau \geqslant 0.1$, they are unimodal and close to a Gaussian. Note that, in our examples, $\alpha = (0.5 - 1.5) \times \tau$.

For $V(2) = 0$, the eigenvalue densities will be a sum of spikes at $0, 2\Delta, 4\Delta, \ldots$ for $+ve$ parity densities and similarly

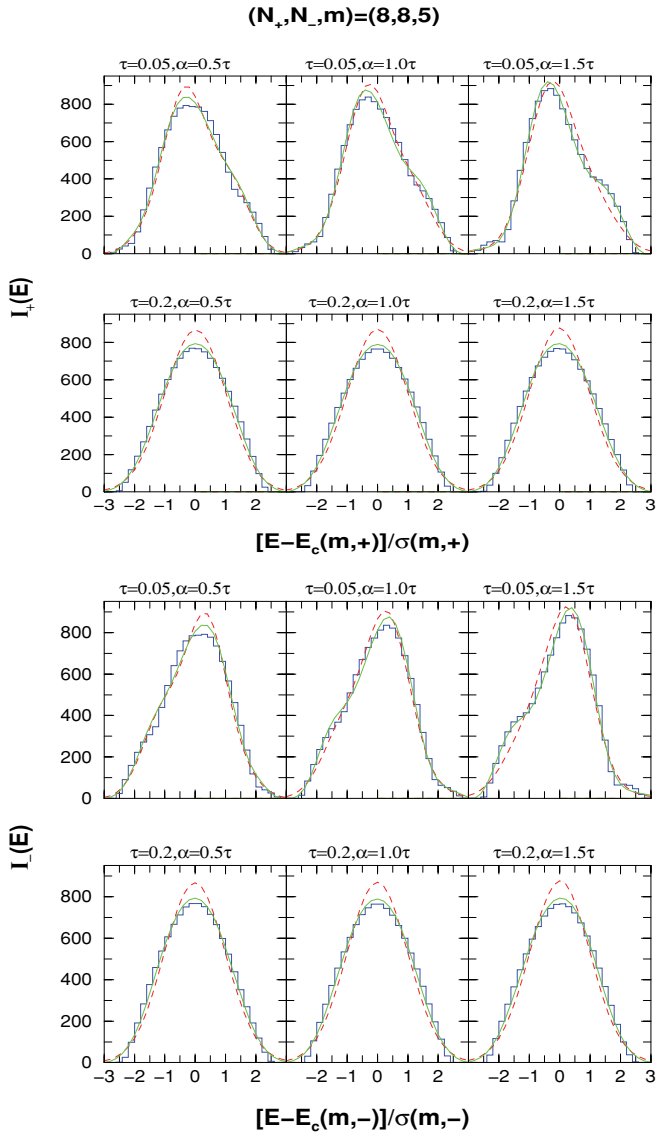

FIG. 3. (Color online) Positive and negative parity state densities for various (τ, α) values for $(N_+, N_-, m) = (8, 8, 5)$ system. Histograms are numerical ensemble results. The dashed (red) curve corresponds to Gaussian form for $\rho^{m_1,m_2}(E)$ in Eq. (16) and, similarly, the solid (green) curve corresponds to Edgeworth corrected Gaussian form with $\gamma_1(m_1, m_2)$ and $\gamma_2(m_1, m_2)$ obtained using the results in Appendix B. See text for details.

at $\Delta, 3\Delta, 5\Delta, \ldots$ for $-ve$ parity densities. As we switch on $V(2)$, the spikes will spread due to the matrices A, B, and C in Fig. 1 and mix due to the matrix D. The variance $\sigma^2(m_1, m_2)$ can be written as

$$\sigma^2(m_1, m_2) = \sigma^2(m_1, m_2 \to m_1, m_2) + \sigma^2(m_1, m_2 \to m_1 \pm 2, m_2 \mp 2). \quad (14)$$

The internal variance $\sigma^2(m_1, m_2 \to m_1, m_2)$ is due to A, B, and C matrices and it receives contribution only from the τ parameter. Similarly, the external variance $\sigma^2(m_1, m_2 \to m_1 \pm 2, m_2 \mp 2)$ is due to the matrix D and it receives contribution only from the α parameter. When we switch on $V(2)$, as the ensemble-averaged centroids generated by $V(2)$ will be zero, the positions of the spikes will be largely unaltered. However, they will start spreading and mixing as τ and α increase. Therefore, the density will be multimodal with the modes well separated for very small (τ, α) values. Some examples for this are shown in Fig. 5. As τ and α start increasing from zero, the spikes spread and will start overlapping for $\sigma(m_1, m_2) \gtrsim \Delta$. This is the situation with $\tau = 0.05$ shown in Figs. 2, 3, and 4. However, as τ increases (with $\alpha \sim \tau$), the densities start becoming unimodal as seen from the $\tau = 0.1$ and 0.2 examples. Also, the m dependence is not strong as seen from Figs. 2, 3, and 4. Now we will discuss the comparison of the ensemble results with the smoothed densities constructed using $E_c(m_1, m_2)$, $\sigma^2(m_1, m_2)$, $\gamma_1(m_1, m_2)$, and $\gamma_2(m_1, m_2)$.

As the particle numbers in the examples shown in Figs. 2, 3, and 4 are small, the excess parameter $\gamma_2(m, \pi) \sim -0.7$ to -0.8 [skewness parameter $\gamma_1(m, \pi) \sim 0$ in all our examples]. Therefore, the densities are not very close to a Gaussian form. It has been well established that the ensemble-averaged eigenvalue density takes Gaussian form in the case of spinless fermion (as well as boson) systems and also for the embedded ensembles extending to those with good quantum numbers (see [3,9,14,18] and references therein). Thus, it can be anticipated that Gaussian form is generic for the state densities or, more appropriately, for the partial densities $\rho^{m_1,m_2}(E)$ generated by EGOE$(1+2)$-π for some range of (τ, α) values. Results for the fixed-π densities for $(N_+, N_-, m) = (8, 8, 6)$, $(6, 10, 6)$, and $(10, 6, 6)$ systems are shown in Fig. 6. The smoothed $+ve$ and $-ve$ parity densities are a sum of the partial densities $\rho^{m_1,m_2}(E)$:

$$\rho_\pm(E) = \frac{1}{d_\pm} \sum_{m_1,m_2}{}' d(m_1, m_2) \rho^{m_1,m_2}(E). \quad (15)$$

Note that the summation in Eq. (15) is over m_2 even for $+ve$ parity density and similarly over m_2 odd for $-ve$ parity density. Here, $\rho_\pm(E)$ as well as $\rho^{m_1,m_2}(E)$ are normalized to unity. However, in practice, the densities normalized to dimensions are needed and they are denoted, as used earlier, by $I_\pm(E)$ and $I^{m_1,m_2}(E)$, respectively:

$$I_\pm(E) = d_\pm \rho_\pm(E) = \sum_{m_1,m_2}{}' I^{m_1,m_2}(E), \qquad I^{m_1,m_2}(E) = d(m_1, m_2) \rho^{m_1,m_2}(E). \quad (16)$$

We employ the Edgeworth (ED) form that includes γ_1 and γ_2 corrections to the Gaussian partial densities $\rho_{\mathcal{G}}^{m_1,m_2}(E)$. Then,

$$\rho^{m_1,m_2}(E) \to \rho_{\mathcal{G}}^{m_1,m_2}(E) \to \rho_{ED}^{m_1,m_2}(E)$$

and, in terms of the standardized variable $\widehat{E}$, the ED form is given by

$$\eta_{\rm ED}(\widehat{E}) = \eta_{\mathcal{G}}(\widehat{E}) \left\{ 1 + \left[\frac{\gamma_1}{6} He_3(\widehat{E}) \right] + \left[\frac{\gamma_2}{24} He_4(\widehat{E}) + \frac{\gamma_1^2}{72} He_6(\widehat{E}) \right] \right\}, \quad (17)$$

$$\eta_{\mathcal{G}}(\widehat{E}) = \frac{1}{\sqrt{2\pi}} \exp\left(-\frac{\widehat{E}^2}{2} \right).$$

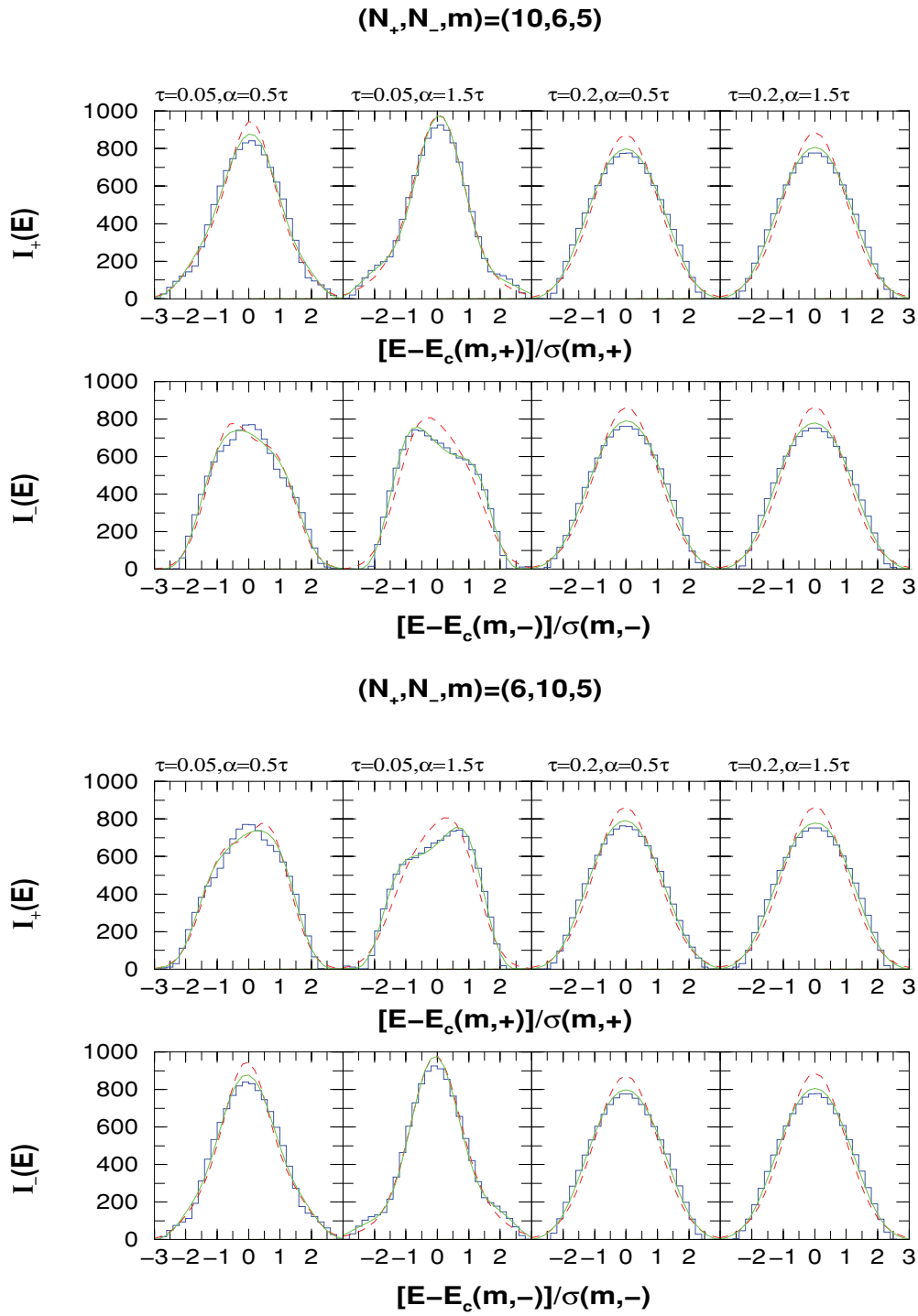

FIG. 4. (Color online) Positive and negative parity state densities for various (τ, α) values for $(N_+, N_-, m) = (10, 6, 5)$ and $(6, 10, 5)$ systems. Histograms are numerical ensemble results. The dashed (red) curve corresponds to Gaussian form for $\rho^{m_1,m_2}(E)$ in Eq. (16) and, similarly, the solid (green) curve corresponds to Edgeworth corrected Gaussian form with $\gamma_1(m_1, m_2)$ and $\gamma_2(m_1, m_2)$ obtained using the results in Appendix B. See text for details.

Here, He are Hermite polynomials: $He_3(x) = x^3 - 3x$, $He_4(x) = x^4 - 6x^2 + 3$, and $He_6(x) = x^6 - 15x^4 + 45x^2 - 15$. By using Eqs. (15) and (17) with exact centroids and variances given by the propagation formulas in Sec. III and the binary correlation results for γ_1 and γ_2 as given by the formulas in Appendix B, the smoothed $+ve$ and $-ve$ parity state densities are constructed. We set $\eta_{\rm ED}(\widehat{E}) = 0$ when $\eta_{\rm ED}(\widehat{E}) < 0$. It is clearly seen from Fig. 6 that the sum of partial densities, with the partial densities represented by ED corrected Gaussians, describes extremely well the exact fixed-π densities in these examples. Therefore, for the (τ, α) values in the range determined by nuclear $sdfp$ and $fpg_{9/2}$

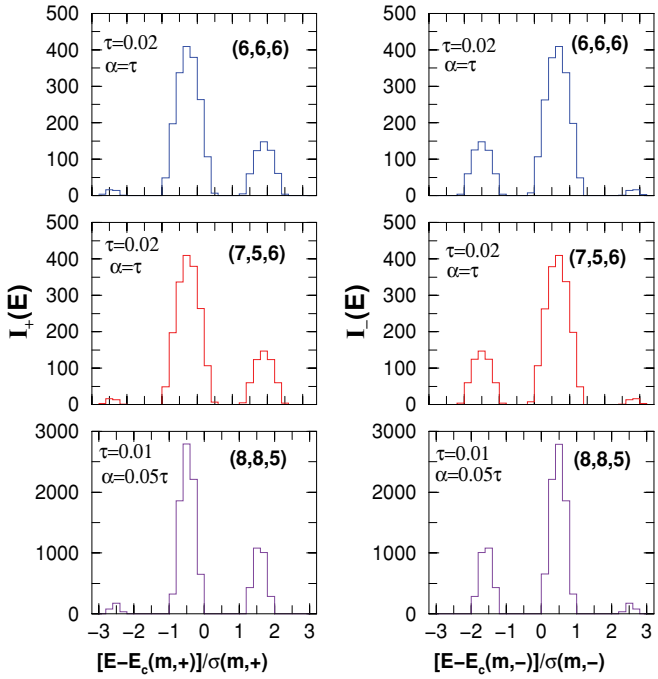

FIG. 5. (Color online) Positive and negative parity state densities for some small values of (τ, α). The (N_+, N_-, m) values are given in the figures. See text for details.

interactions, i.e., $\tau \sim 0.1$–0.3 and $\alpha \sim 0.5\tau$–2τ, the partial densities can be well represented by ED corrected Gaussians, and total densities are also close to ED corrected Gaussians. Unlike Fig. 6, densities in Figs. 2, 3, and 4 show, in many cases, strong departures from Gaussian form. Therefore, it is important to test how well Eq. (16) with ED corrected Gaussian for $\rho^{m_1,m_2}(E)$ describes the numerical results for $I_\pm(E)$. We show this comparison for all the densities in Figs. 3 and 4. It is clearly seen that the agreements with ED corrected Gaussians are good in all the cases. Therefore, the large deviations from the Gaussian form for $I_\pm(E)$ arise mainly because of the distribution of the centroids [this involves dimensions of the (m_1, m_2) configurations] of the partial densities involved. It is possible that the agreements in Figs. 3 and 4 may become more perfect if we employ, for the partial densities, some noncanonical forms defined by the first four moments as given, for example, in [48,49]. However, as these forms are not derived using any random matrix ensemble, we have not used these for the partial densities in our present investigation. In conclusion, for the physically relevant range of (τ, α) values, the propagation formulas for centroids and variances given by Eqs. (9) and (10) or, alternatively, with $E_c(m_1, m_2) = m_2\Delta$ and Eq. (12) along with the EGOE$(1+2)$-π ensemble-averaged $\gamma_1(m_1, m_2)$ and $\gamma_2(m_1, m_2)$ formulas (obtained using the binary correlation approximation as given in Appendix B), can be used to construct fixed-π state densities for larger (N_+, N_-, m) systems.

B. Parity ratios for state densities

As stated in the beginning, parity ratio of state densities at a given excitation energy (E) is a quantity of considerable interest in nuclear structure. For the systems shown in Figs. 2, 3, and 4 and also for many other systems, we have studied the parity ratios and the results are shown in Figs. 7–10. As the parity ratios need to be calculated at a given value of excitation energy E, we measure the eigenvalues in both $+ve$ and $-ve$ parity spaces with respect to the absolute ground-state energy E_{gs} of the $N = N_+ + N_-$ system. Thus, E_{gs} is defined by taking all the $+ve$ and $-ve$ parity eigenvalues of all members of the ensemble and choosing the lowest of all these. The ground-state energy can also be determined by averaging the $+ve$ and $-ve$ parity ground-state energies over the ensemble, and then the ground-state energy is the minimum of the two. It is seen that the results for parity ratios are essentially independent of the choice of E_{gs} and, thus, we employ absolute ground-state energy in our calculations. We use the ensemble-averaged total ($+ve$ and $-ve$ eigenvalues combined) spectrum width σ_t of the system for scaling. The total widths σ_t can be calculated also by using $E_c(m_1, m_2)$ and $\sigma^2(m_1, m_2)$. Examples for σ_t are shown in Table II and they are in good agreement with the results obtained using the simple formula given by Eq. (12). We use the variable $\boldsymbol{E} = (E - E_{gs})/\sigma_t$ for calculating parity ratios. Starting with E_{gs} and using a bin size of $\Delta\boldsymbol{E} = 0.2$, we have calculated the number of states $I_+(\boldsymbol{E})$ with $+ve$ parity and also the number of states $I_-(\boldsymbol{E})$ with $-ve$ parity in a given bin, and then the ratio $I_-(\boldsymbol{E})/I_+(\boldsymbol{E})$ is the parity ratio. Note that the results in Figs. 7–10 are shown for $\boldsymbol{E} = 0 - 3$ as the spectrum span is $\sim 5.5\sigma_t$. To go beyond the middle of the spectrum, for real nuclei, one has to include more sp levels (also a finer splitting of the $+ve$ and $-ve$ parity levels may be needed) and, therefore, N_+ and N_- change. Continuing with this, one obtains the Bethe form for nuclear level densities [15].

General observations from Figs. 7–10 are as follows. (i) The parity ratio $I_-(\boldsymbol{E})/I_+(\boldsymbol{E})$ will be zero up to an energy $\boldsymbol{E}_0$. (ii) Then, it starts increasing and becomes larger than unity at an energy $\boldsymbol{E}_m$. (iii) From here on, the parity ratio decreases and saturates quickly to unity from an energy $\boldsymbol{E}_1$. In these examples, $\boldsymbol{E}_0 \lesssim 0.4$, $\boldsymbol{E}_m \sim 1$, and $\boldsymbol{E}_1 \sim 1.5$. It is seen that the curves shift toward left as τ increases. Also, the position of the peak shifts to much larger value of $\boldsymbol{E}_m$ and equilibration gets delayed as α increases for a fixed τ value. Therefore, for larger τ, the energies $(\boldsymbol{E}_0, \boldsymbol{E}_m, \boldsymbol{E}_1)$ are smaller compared to those for a smaller τ. The three transition energies also depend on (N_+, N_-, m). We have also verified, as shown in Fig. 9, that the general structure of the parity ratios will remain the same even when we change $\Delta \to -\Delta$ (i.e., $-ve$ parity sp states below the $+ve$ parity sp states). For the $(N_+, N_-, m) = (8, 8, 4)$ system, results for $\Delta = 1$ are given in Fig. 7 and they are almost the same as the results with $\Delta = -1$ given in Fig. 9. The general structures (i)–(iii) are clearly seen in the numerical examples shown in [25], where a method based on the Fermi-gas model has been employed. If $\sigma_t \sim 6$–8 MeV, equilibration in parities is expected around $E \sim 8$–10 MeV, and this is clearly seen in the examples in [25]. It is also seen from Fig. 8 that the equilibration is quite poor for very small values of τ and, therefore, by comparing with the results in [25], it can be argued that very small values of τ are ruled out for nuclei. Hence, it is plausible to conclude that generic results for parity

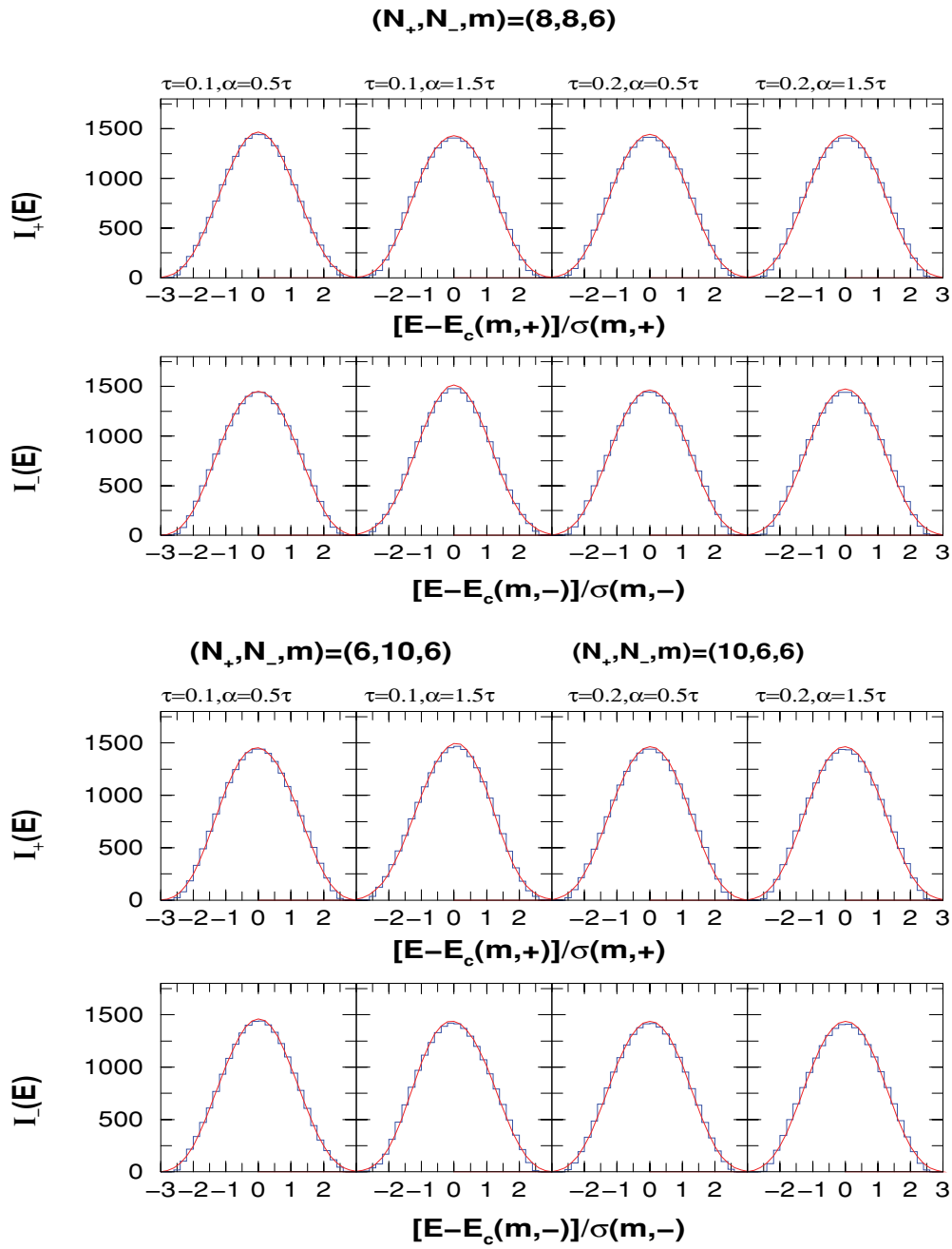

FIG. 6. (Color online) Positive and negative parity state densities for various (τ, α) values for $(N_+, N_-, m) = (8, 8, 6)$, (6, 10, 6), and (10, 6, 6) systems. Smoothed curves (solid red lines) are obtained using fixed-(m_1, m_2) partial densities. See text for details.

ratios can be derived using EGOE$(1 + 2)$-π with reasonably large (τ, α) values. Let us add that the interpretations in [25] are based on the occupancies of the sp orbits, while in this paper, they are in terms of τ and α parameters.

By using the smoothed $I^{\pm}(\boldsymbol{E})$, constructed as discussed in Sec. IV A, smoothed forms for parity ratios are calculated as follows. Starting with the absolute ground-state energy E_{gs} and using a bin size of $\Delta \boldsymbol{E} = 0.2$, $+ve$ and $-ve$ parity densities in a given energy bin are obtained and their ratio is the parity ratio at a given $\boldsymbol{E}$. We have chosen the examples where I_+ and I_- are close to Gaussians. It is seen from Fig. 10 that the agreement with exact results is good for $\boldsymbol{E} \gtrsim 0.5$. However, for smaller $\boldsymbol{E}$, to obtain a good agreement, one should have a better prescription for determining the tail part of the $\rho^{m_1,m_2}(\boldsymbol{E})$ distributions. Developing the theory for this is beyond the scope of this paper as this requires more complete analytical treatment of the ensemble.

C. Probability for $+ve$ parity ground states

Papenbrock and Weidenmüller used the $\tau \to \infty$, $\alpha = \tau$ limit of EGOE$(1 + 2)$-π for several (N_+, N_-, m) systems

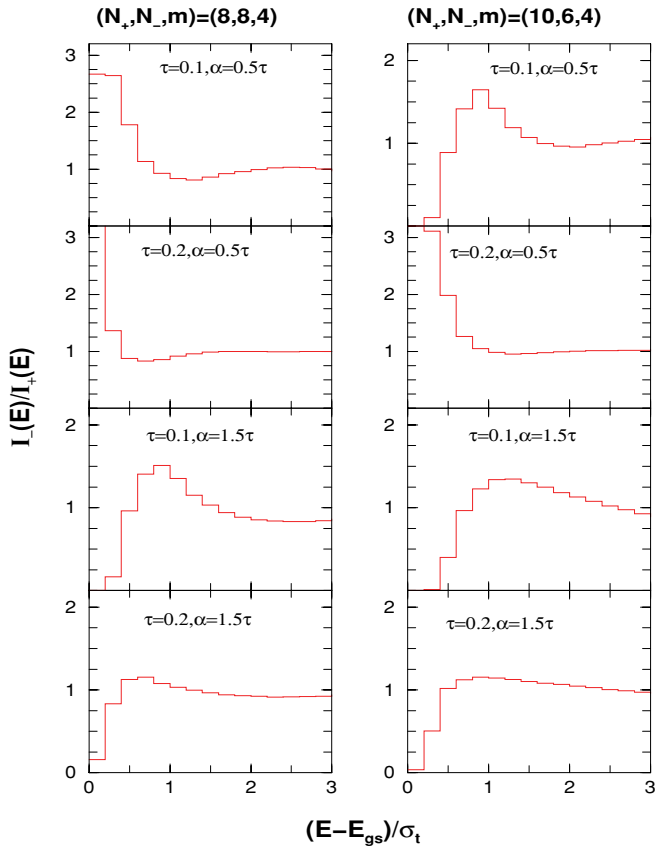

FIG. 7. (Color online) Parity ratios for various (τ, α) values for $(N_+, N_-, m) = (8, 8, 4)$ and $(10, 6, 4)$ systems. See text for details.

to study the probability (R_+) for $+ve$ parity ground states over the ensemble [29]. As stated before, this exercise was motivated by shell-model results with random interaction giving preponderance of $+ve$ parity ground states [28]. The numerical calculations in [29] showed considerable variation (18%−84%) in R_+. In addition, they gave a plausible proof that, in the dilute limit $[m \ll (N_+, N_-)]$, R_+ will approach 50%. Combining these, they argued that the observed preponderance of $+ve$ parity ground states could be a finite size (finite N_+, N_-, m) effect. For the extended EGOE$(1 + 2)$-π considered in this paper, where the $\tau \to \infty$ and $\alpha = \tau$ restriction is relaxed, as we will discuss now, R_+ can reach 100%.

For EGOE$(1 + 2)$-π with $\tau \sim 0$, clearly one will get $R_+ = 100\%$ (for even m and $m \ll N_+, N_-$) and, therefore, it is of interest to study R_+ variation with (τ, α). We have carried out calculations using a 200-member ensemble for $(N_+, N_-, m) = (6, 6, 6)$ and 100-member ensembles for $(8, 8, 5)$, $(6, 6, 6)$, $(6, 10, 4)$, and $(6, 10, 5)$ systems. In these calculations, we use $\alpha = \tau$ and 1.5τ. The results are shown in Fig. 11. For $\alpha = \tau$, the results are as follows. For $\tau \lesssim 0.04$, we have $R_+ \sim 100\%$ and then R_+ starts decreasing with some fluctuations between $\tau = 0.1$ and 0.2. The origin of these fluctuations is not clear. As $\tau > 1$ is not realistic, we have restricted the R_+ calculations to $\tau \leqslant 1$. We see from the figure that EGOE$(1 + 2)$-π generates $R_+ \gtrsim 50\%$ for $\tau \leqslant 0.3$ independent of (N_+, N_-, m). Also, R_+ decreases much faster with τ and reaches ∼30% for $\tau = 0.5$ for $(N_+, N_-, m) = (6, 6, 6)$. For $m < (N_+, N_-)$, the decrease in R_+ is slower. If we increase α, from the structure of the two-particle H matrix in Fig. 1, we can easily infer that the width of the lowest $+ve$ parity (m_1, m_2) unitary configuration becomes much larger compared to the lowest $-ve$ parity unitary configuration (see Table II for examples). Therefore, with increasing α, we expect R_+ to increase and this is clearly seen in Fig. 11. Thus, $\alpha \gtrsim \tau$ is required for R_+ to be large. A quantitative description of R_+ requires the construction of $+ve$ and $-ve$ parity state densities more accurately in the tail region and the theory for this is not yet available.

V. CONCLUSIONS AND FUTURE OUTLOOK

In this paper, we have introduced a generalized EGOE$(1 + 2)$-π ensemble for identical fermions and its construction follows from EGOE$(1 + 2)$ for spinless fermion systems. Using this generalized EE, we have not only studied R_+, as it was done by Papenbrock and Weidenmüller [29] using a simpler two-body ensemble with parity, but also studied the form of fixed-π state densities and parity ratios, which are important nuclear structure quantities. Numerical examples (see Figs. 2–4 and 6), with the range of the various parameters in the model fixed using realistic nuclear effective interactions, are used to show that the fixed-π state densities in finite-dimensional spaces are of Gaussian form for sufficiently large values of the mixing parameters (τ, α). The random matrix model also captures the essential features of parity ratios as seen in the method based on noninteracting Fermi-gas model reported in [25]. We also found preponderance of $+ve$ parity ground states for $\tau \lesssim 0.5$ and $\alpha \sim 1.5\tau$. In addition, for constructing fixed-π Gaussian densities, we have derived an easy to understand propagation formula [see Eq. (10)] for the spectral variances of the partial densities $\rho^{m_1,m_2}(E)$ that generate I_+ and I_-. Similarly, for calculating the corrections to the Gaussian forms, formulas for skewness γ_1 and excess γ_2 of the partial densities $\rho^{m_1,m_2}(E)$ are derived using the binary correlation approximation (see Appendix B for the formulas). The smoothed densities constructed using Edgeworth corrected Gaussians are shown to describe the numerical results for $I_\pm(E)$ [for (τ, α) values in the range defined by nuclear $sdfp$ and $fpg_{9/2}$ interactions (see beginning of Sec. IV)] and also the parity ratios at energies away from the ground state. Numerical results presented for parity ratios at lower energies show that a better theory for the tails of the partial densities is needed (see Figs. 7–10). Thus, the results in this paper represent considerable progress in analyzing the EGOE$(1 + 2)$-π ensemble, going much beyond the analysis presented in [29].

The results in this paper are largely numerical and they clearly show that developing a complete analytical theory, going beyond the results presented in Sec. III and Appendix B, for EGOE$(1 + 2)$-π is important. In the future, it is important to investigate EGOE$(1 + 2)$-π for proton-neutron systems and then we will have four unitary orbits (two for protons and two for neutrons). In addition, by including nondegenerate $+ve$ and $-ve$ parity sp states, the model could be applied to nuclei for

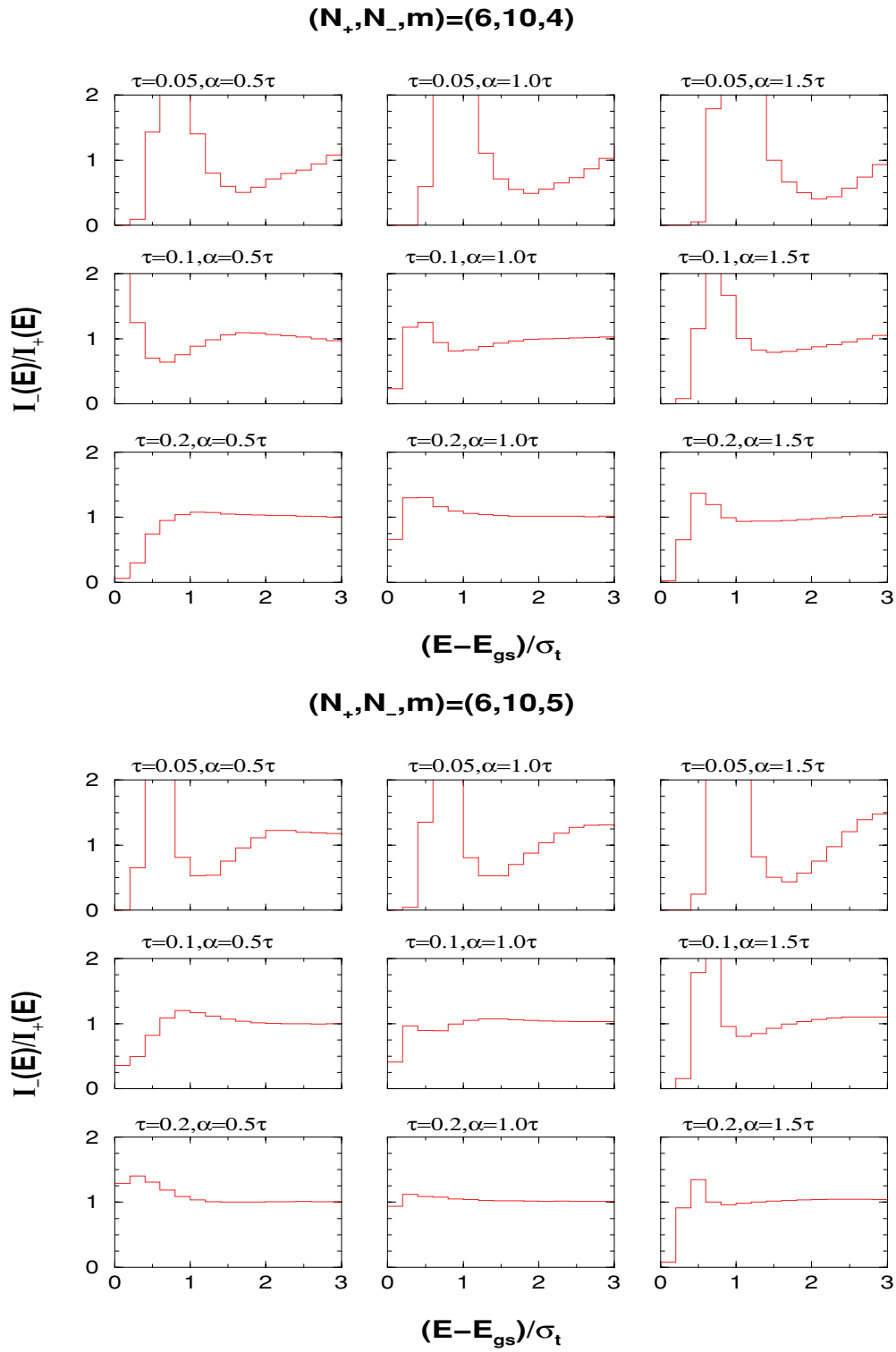

FIG. 8. (Color online) Parity ratios for various (τ, α) values for $(N_+, N_-, m) = (6, 10, 4)$ and $(6, 10, 5)$ systems. See text for details.

predicting parity ratios. This extended EGOE$(1 + 2)$-π model with protons and neutrons occupying different sp states will be generated by a 10×10 block matrix for $V(2)$ in two-particle spaces. Therefore, parametrization of this ensemble is more complex. Analysis of this extended EGOE$(1 + 2)$-π is for the future.

ACKNOWLEDGMENTS

All the calculations in this paper were carried out using the HPC cluster resource at Physical Research Laboratory. Thanks are due to E.R. Prahlad and G. Vignesh for collaboration in the initial stages. Thanks are also due to S. Tomsovic for

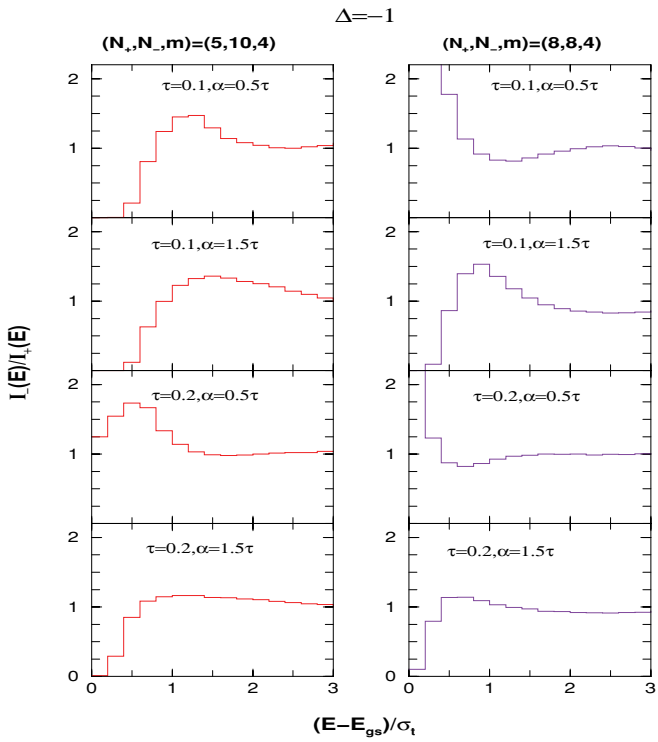

FIG. 9. (Color online) Parity ratios for some values of (τ, α) with $\Delta = -1$ for $(N_+, N_-, m) = (5, 10, 4)$ and $(8, 8, 4)$ systems. See text for details.

some useful discussions and to the referee for some useful comments.

APPENDIX A

Let us consider a system of m fermions in N sp states with a $(1+2)$-body Hamiltonian $H = h(1) + V(2)$, where $h(1) = \sum_i \epsilon_i \hat{n}_i$ and $V(2)$ is defined by the two-body matrix elements $V_{ijkl} = \langle kl|V(2)|ij\rangle$. With respect to the $U(N)$ group, the two-body interaction $V(2)$ can be separated into scalar ($\nu = 0$), effective one-body ($\nu = 1$), and irreducible two-body ($\nu = 2$) parts [14,15,30,36]:

$$
\begin{aligned}
V^{\nu=0} &= \frac{\hat{n}(\hat{n}-1)}{2}\overline{V}, \quad \overline{V} = \binom{N}{2}^{-1}\sum_{i<j} V_{ijij},\\
V^{\nu=1} &= \frac{\hat{n}-1}{N-2}\sum_{i,j}\zeta_{i,j}a_i^\dagger a_j,\\
\zeta_{i,j} &= \left[\sum_k V_{kikj}\right] - \left[(N)^{-1}\sum_{r,s} V_{rsrs}\right]\delta_{i,j},\\
V^{\nu=2} &= V - V^{\nu=0} - V^{\nu=1} \Longleftrightarrow V^{\nu=2}_{ijkl},\\
V^{\nu=2}_{ijij} &= V_{ijij} - \overline{V} - (N-2)^{-1}(\zeta_{i,i} + \zeta_{j,j}),\\
V^{\nu=2}_{ijik} &= V_{ijik} - (N-2)^{-1}\zeta_{j,k} \quad \text{for } j \neq k,\\
V^{\nu=2}_{ijkl} &= V_{ijkl} \ \text{ for all other cases.}
\end{aligned}
\tag{A1}
$$

Similar to Eq. (A1), the $h(1)$ operator will have $\nu = 0, 1$ parts,

$$
\begin{aligned}
h^{\nu=0} &= \overline{\epsilon}\hat{n}, \quad \overline{\epsilon} = (N)^{-1}\sum_i \epsilon_i,\\
h^{\nu=1} &= \sum_i \epsilon_i^1 \hat{n}_i, \quad \epsilon_i^1 = \epsilon_i - \overline{\epsilon}.
\end{aligned}
\tag{A2}
$$

Then, the propagation equations for the m-particle centroids and variances are [14,15,30,36]

$$
\begin{aligned}
E_c(m) &= \langle H\rangle^m = m\,\overline{\epsilon} + \binom{m}{2}\overline{V},\\
\sigma^2(m) &= \langle H^2\rangle^m - [E_c(m)]^2\\
&= \frac{m(N-m)}{N(N-1)}\sum_{i,j}\left\{\epsilon_i^1\delta_{i,j} + \frac{m-1}{N-2}\zeta_{i,j}\right\}^2\\
&\quad + \frac{m(m-1)(N-m)(N-m-1)}{N(N-1)(N-2)(N-3)}\langle\langle (V^{\nu=2})^2\rangle\rangle^2.
\end{aligned}
\tag{A3}
$$

APPENDIX B

For the EGOE$(1+2)$-π Hamiltonian defined in Eq. (1), we have $H = h(1) + V(2) = h(1) + X(2) + D(2)$ with $X(2) = A \oplus B \oplus C$ is the direct sum of the spreading matrices A, B, and C, and $D(2) = D + \widetilde{D}$ is the off-diagonal mixing matrix as shown in Fig. 1. Here, $\widetilde{D}$ is the transpose of the matrix D. With the sp energies defining the mean field $h(1)$ as given in Eq. (1), the first moment M_1 of $\rho^{m_1,m_2}(E)$ is, trivially,

$$
M_1(m_1, m_2) = \overline{\langle (h+V)\rangle^{m_1,m_2}} = m_2, \tag{B1}
$$

as $\langle h^r\rangle^{m_1,m_2} = (m_2)^r$ and $\overline{\langle V\rangle^{m_1,m_2}} = 0$. By extending the binary correlation method to traces over two-orbit configurations, we have derived formulas for the second-, third-, and fourth-order traces giving $M_r(m_1, m_2), r = 2$–4. It is important to mention that the presence of the mixing matrix D makes the derivations lengthy. Therefore, we give only the final formulas in this paper and discuss elsewhere the details of the derivations [44]. The second moment M_2 is

$$
\begin{aligned}
M_2(m_1, m_2) &= \overline{\langle (h+V)^2\rangle^{m_1,m_2}} = \langle h^2\rangle^{m_1,m_2} + \overline{\langle V^2\rangle^{m_1,m_2}}\\
&= (m_2)^2 + \mathcal{X}(m_1, m_2) + \mathcal{D}(m_1, m_2)\\
&\quad + \widetilde{\mathcal{D}}(m_1, m_2),\\
\mathcal{X}(m_1, m_2) &= \overline{\langle X^2\rangle^{m_1,m_2}} = \tau^2\sum_{i+j=2}\binom{\widetilde{m}_1+i}{i}\binom{m_1}{i}\\
&\quad \times\binom{\widetilde{m}_2+j}{j}\binom{m_2}{j},\\
\mathcal{D}(m_1, m_2) &= \overline{\langle D\widetilde{D}\rangle^{m_1,m_2}} = \alpha^2\binom{m_1}{2}\binom{\widetilde{m}_2}{2},\\
\widetilde{\mathcal{D}}(m_1, m_2) &= \overline{\langle \widetilde{D}D\rangle^{m_1,m_2}} = \alpha^2\binom{\widetilde{m}_1}{2}\binom{m_2}{2}.
\end{aligned}
\tag{B2}
$$

Here, for brevity, we have defined $\mathcal{X}(m_1, m_2) = \overline{\langle X^2\rangle^{m_1,m_2}}$, $\mathcal{D}(m_1, m_2) = \overline{\langle D\widetilde{D}\rangle^{m_1,m_2}}$, and $\widetilde{\mathcal{D}}(m_1, m_2) = \overline{\langle \widetilde{D}D\rangle^{m_1,m_2}}$. Note

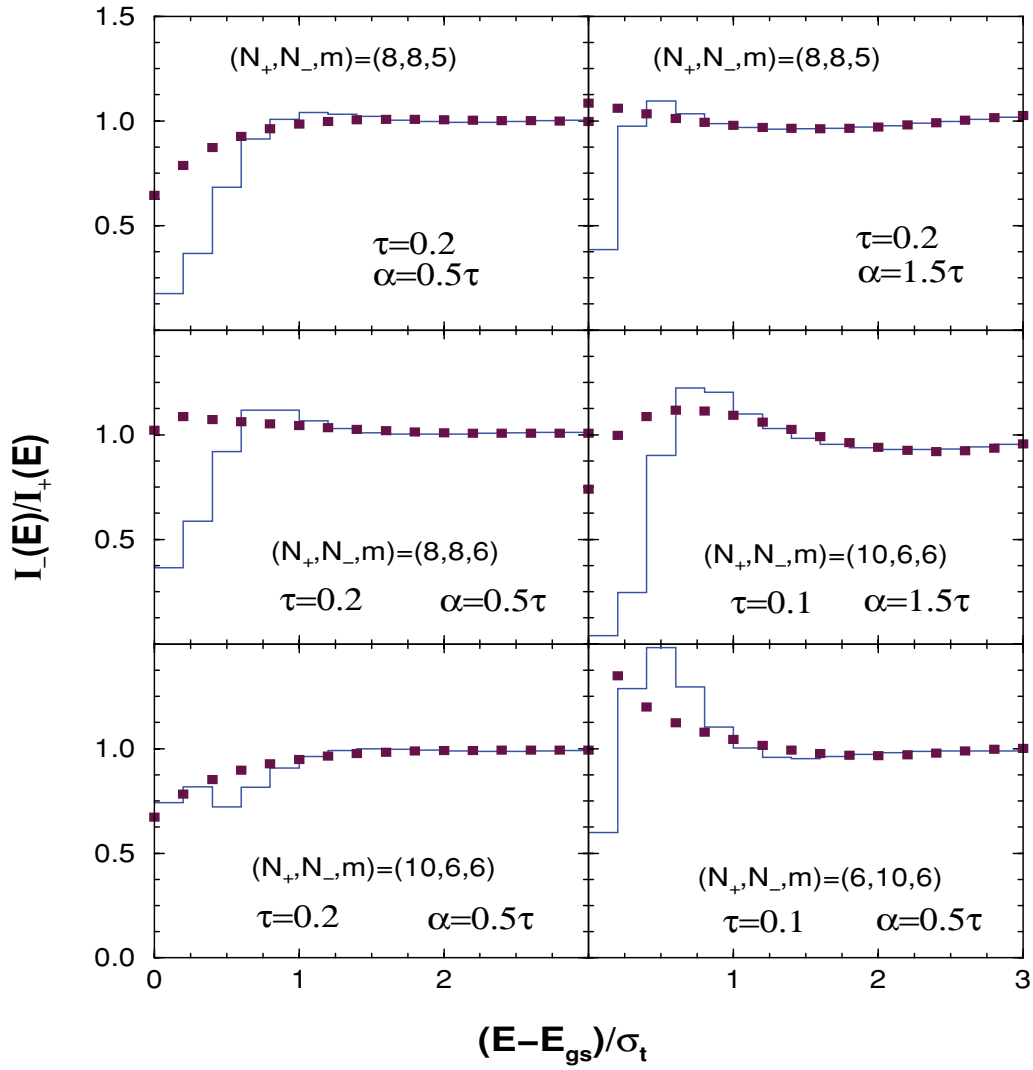

FIG. 10. (Color online) Parity ratios for various (τ, α) values and for various (N_+, N_-, m) systems. Histograms are the ensemble results. Filled squares (brown) are obtained using fixed-(m_1, m_2) ED corrected Gaussian partial densities, i.e., the $I_\pm(E)$ are obtained using Eq. (16) with $\rho_{\rm ED}^{m_1,m_2}(E)$. The $\gamma_1(m_1, m_2)$ and $\gamma_2(m_1, m_2)$ parameters defining $\rho_{\rm ED}^{m_1,m_2}(E)$ are calculated using Eqs. (B2)–(B7). See text for further details.

that Eq. (B2) gives the binary correlation formula for $\overline{\sigma^2(m_1, m_2)}$ and it reduces to Eq. (12) as expected. Similarly, the third moment M_3 is

$$M_3(m_1, m_2) = \overline{\langle (h+V)^3\rangle^{m_1,m_2}} = \langle h^3\rangle^{m_1,m_2} + 2\langle h\rangle^{m_1,m_2}\overline{\langle V^2\rangle^{m_1,m_2}} + \overline{\langle XhX\rangle^{m_1,m_2}} + \overline{\langle Dh\widetilde{D}\rangle^{m_1,m_2}} + \overline{\langle \widetilde{D}hD\rangle^{m_1,m_2}}$$
$$= (m_2)^3 + 3(m_2)\mathcal{X}(m_1, m_2) + (3m_2+2)\mathcal{D}(m_1, m_2) + (3m_2-2)\widetilde{\mathcal{D}}(m_1, m_2). \quad \text{(B3)}$$

The formula for the fourth moment M_4 is

$$M_4(m_1, m_2) = \overline{\langle (h+V)^4\rangle^{m_1,m_2}} = \langle h^4\rangle^{m_1,m_2} + 3\langle h^2\rangle^{m_1,m_2}\overline{\langle V^2\rangle^{m_1,m_2}} + \langle h^2\rangle^{m_1,m_2}\overline{\langle X^2\rangle^{m_1,m_2}} + \overline{\langle Dh^2\widetilde{D}\rangle^{m_1,m_2}}$$
$$+ \overline{\langle \widetilde{D}h^2D\rangle^{m_1,m_2}} + 2\overline{\langle hXhX\rangle^{m_1,m_2}} + 2\overline{\langle hDh\widetilde{D}\rangle^{m_1,m_2}} + 2\overline{\langle h\widetilde{D}hD\rangle^{m_1,m_2}} + \overline{\langle V^4\rangle^{m_1,m_2}}$$
$$= (m_2)^4 + 6(m_2)^2\mathcal{X}(m_1, m_2) + [6(m_2)^2 + 8(m_2) + 4]\mathcal{D}(m_1, m_2) + [6(m_2)^2 - 8(m_2) + 4]\widetilde{\mathcal{D}}(m_1, m_2) + \overline{\langle V^4\rangle^{m_1,m_2}}. \quad \text{(B4)}$$

TABLE III. Exact results for skewness and excess parameters for fixed-π eigenvalue densities $I_{\pm}(E)$ compared with the binary correlation results (in the table, called Approx.). For exact results, we have used the eigenvalues obtained from EGOE(1 + 2)-π ensembles with 100 members. The binary correlation results are obtained using Eqs. (B1)–(B8) and extension of Eq. (11). See text for details.

(N_+, N_-, m)	$(\tau, \alpha/\tau)$	$\gamma_1(m,\pi)$				$\gamma_2(m,\pi)$			
		Exact		Approx.		Exact		Approx.	
		$\pi=+$	$\pi=-$	$\pi=+$	$\pi=-$	$\pi=+$	$\pi=-$	$\pi=+$	$\pi=-$
(8, 8, 5)	(0.05, 0.5)	0.15	−0.15	0.15	−0.15	−0.52	−0.52	−0.52	−0.52
	(0.05, 1.0)	0.16	−0.16	0.16	−0.16	−0.50	−0.50	−0.50	−0.50
	(0.05, 1.5)	0.18	−0.17	0.18	−0.18	−0.46	−0.46	−0.46	−0.46
	(0.2, 0.5)	−0.03	0.03	−0.03	0.03	−0.71	−0.71	−0.71	−0.71
	(0.2, 1.0)	−0.01	0.01	−0.01	0.01	−0.73	−0.73	−0.74	−0.74
	(0.2, 1.5)	0.02	−0.02	0.02	−0.02	−0.72	−0.72	−0.73	−0.73
(10, 6, 5)	(0.05, 0.5)	−0.06	0.09	−0.07	0.09	−0.26	−0.76	−0.26	−0.75
	(0.05, 1.5)	−0.04	0.15	−0.05	0.15	−0.01	−0.86	−0.01	−0.86
	(0.2, 0.5)	0.01	−0.04	0.01	−0.04	−0.73	−0.69	−0.73	−0.69
	(0.2, 1.5)	0.01	0.02	0.01	0.02	−0.69	−0.75	−0.70	−0.75
(6, 10, 5)	(0.05, 0.5)	−0.09	0.07	−0.09	0.07	−0.76	−0.26	−0.75	−0.26
	(0.05, 1.5)	−0.15	0.05	−0.15	0.05	−0.86	−0.01	−0.86	−0.01
	(0.2, 0.5)	0.04	−0.01	0.04	−0.01	−0.68	−0.73	−0.69	−0.73
	(0.2, 1.5)	−0.02	−0.01	−0.02	−0.01	−0.75	−0.69	−0.75	−0.70

The only unknown in Eq. (B4) is $\overline{\langle V^4\rangle^{m_1,m_2}}$ and the expression for this is complicated:

$$\begin{aligned}\overline{\langle V^4\rangle^{m_1,m_2}} &= \overline{\langle X^4\rangle^{m_1,m_2}} + 3\overline{\langle X^2\rangle^{m_1,m_2}}\{\overline{\langle D\widetilde{D}\rangle^{m_1,m_2}} + \overline{\langle \widetilde{D}D\rangle^{m_1,m_2}}\} + \overline{\langle DX^2\widetilde{D}\rangle^{m_1,m_2}} \\ &\quad + \overline{\langle \widetilde{D}X^2D\rangle^{m_1,m_2}} + 2\overline{\langle XDX\widetilde{D}\rangle^{m_1,m_2}} + 2\overline{\langle X\widetilde{D}XD\rangle^{m_1,m_2}} + \overline{\langle (D+\widetilde{D})^4\rangle^{m_1,m_2}} \\ &= 2[\mathcal{X}(m_1,m_2)]^2 + 3[\mathcal{X}(m_1,m_2)][\mathcal{D}(m_1,m_2) + \widetilde{\mathcal{D}}(m_1,m_2)] + T_1(m_1,m_2) \\ &\quad + T_2(m_1,m_2) + 2T_3(m_1,m_2) + T_4(m_1,m_2), \end{aligned} \tag{B5}$$

where

$$\begin{aligned} T_1(m_1,m_2) &= \tau^4 \sum_{i+j=2,t+u=2} F(m_1,N_1,i,t)F(m_2,N_2,j,u), \\ F(m,N,k_1,k_2) &= \sum_{s=0}^{k_2} \binom{m-s}{k_2-s}^2 \binom{N-m+k_1-s}{k_1}\binom{m-s}{k_1}\binom{N-m}{s}\binom{m}{s}\binom{N+1}{s}\frac{N-2s+1}{N-s+1}\binom{N-s}{k_2}^{-1}\binom{k_2}{s}^{-1}, \\ T_2(m_1,m_2) &= \mathcal{D}(m_1,m_2)\mathcal{X}(m_1-2,m_2+2) + \widetilde{\mathcal{D}}(m_1,m_2)\mathcal{X}(m_1+2,m_2-2), \\ T_3(m_1,m_2) &= \tau^2\alpha^2 \sum_{i+j=2}\left[\binom{m_1-i}{2}\binom{\widetilde{m}_2-j}{2} + \binom{\widetilde{m}_1-i}{2}\binom{m_2-j}{2}\right]\binom{\widetilde{m}_1+i}{i}\binom{m_1}{i}\binom{\widetilde{m}_2+j}{j}\binom{m_2}{j}, \\ T_4(m_1,m_2) &= [\mathcal{D}(m_1,m_2)]^2 + [\widetilde{\mathcal{D}}(m_1,m_2)]^2 + \mathcal{D}(m_1,m_2)[2\mathcal{D}(m_1-2,m_2+2) + \widetilde{\mathcal{D}}(m_1-2,m_2+2)] \\ &\quad + \widetilde{\mathcal{D}}(m_1,m_2)[2\widetilde{\mathcal{D}}(m_1+2,m_2-2) + \mathcal{D}(m_1+2,m_2-2)] + 4\mathcal{D}(m_1,m_2)\widetilde{\mathcal{D}}(m_1,m_2). \end{aligned} \tag{B6}$$

Given the moments $M_r(m_1,m_2) = \overline{\langle H^r\rangle^{m_1,m_2}}$, $r = 1-4$, the skewness and excess parameters γ_1 and γ_2 are as follows [50]:

$$\begin{aligned} \gamma_1(m_1,m_2) &= \frac{k_3(m_1,m_2)}{[k_2(m_1,m_2)]^{3/2}}, \\ \gamma_2(m_1,m_2) &= \frac{k_4(m_1,m_2)}{[k_2(m_1,m_2)]^2}, \end{aligned} \tag{B7}$$

where

$$\begin{aligned} k_2(m_1,m_2) &= M_2(m_1,m_2) - M_1^2(m_1,m_2), \\ k_3(m_1,m_2) &= M_3(m_1,m_2) - 3\,M_2(m_1,m_2)M_1(m_1,m_2) \\ &\quad + 2\,M_1^3(m_1,m_2), \\ k_4(m_1,m_2) &= M_4(m_1,m_2) - 4\,M_3(m_1,m_2)M_1(m_1,m_2) \\ &\quad - 3\,M_2^2(m_1,m_2) + 12\,M_2(m_1,m_2)M_1^2(m_1,m_2) \\ &\quad - 6\,M_1^4(m_1,m_2). \end{aligned} \tag{B8}$$

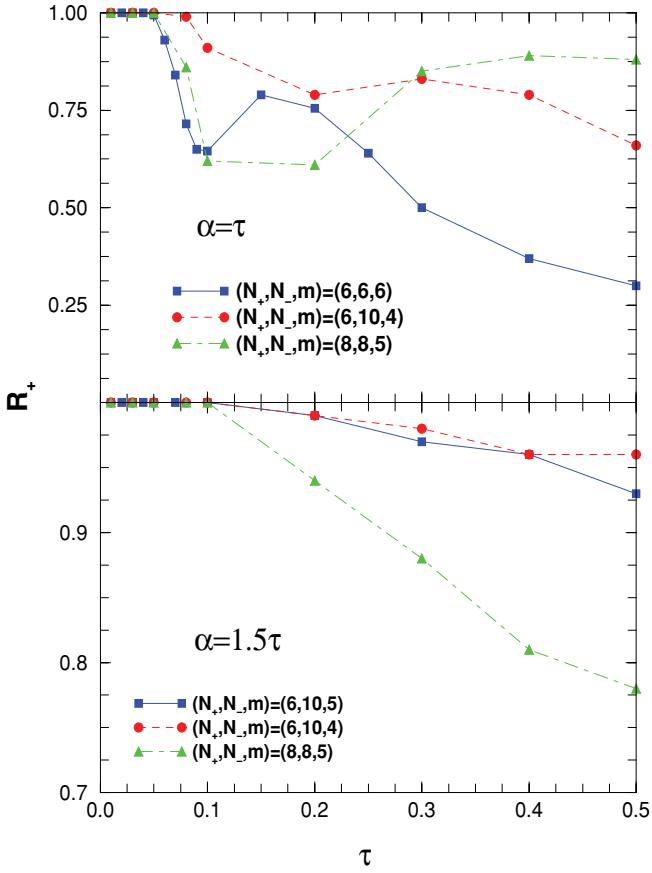

FIG. 11. (Color online) Probability (R_+) for $+ve$ parity ground states for various (τ, α) values and for various (N_+, N_-, m) systems. See text for details.

After carrying out the simplifications using Eqs. (B1)–(B8), it is easily seen that

$$\gamma_1(m_1, m_2) = \frac{2[\mathcal{D}(m_1, m_2) - \widetilde{\mathcal{D}}(m_1, m_2)]}{\{\mathcal{D}(m_1, m_2) + \widetilde{\mathcal{D}}(m_1, m_2) + \mathcal{X}(m_1, m_2)\}^{3/2}}. \tag{B9}$$

The expression for γ_2 is more complex:

$$\begin{aligned}\gamma_2(m_1, m_2) = {} & \{\widetilde{\mathcal{D}}(m_1, m_2) + \mathcal{D}(m_1, m_2) + \mathcal{X}(m_1, m_2)\}^{-2} \\ & \times [T_1(m_1, m_2) + T_2(m_1, m_2) + 2\,T_3(m_1, m_2) \\ & + T_4(m_1, m_2) + [\widetilde{\mathcal{D}}(m_1, m_2) + \mathcal{D}(m_1, m_2)] \\ & \times [4 - \mathcal{X}(m_1, m_2)] - 2[\widetilde{\mathcal{D}}(m_1, m_2) \\ & + \mathcal{D}(m_1, m_2)]^2] - 1. \end{aligned} \tag{B10}$$

With $T_1 \sim [\mathcal{X}(m_1, m_2)]^2 + C_1(m_1, m_2)$, $T_2 = T_3 \sim \mathcal{X}(m_1, m_2)[\widetilde{\mathcal{D}}(m_1, m_2) + \mathcal{D}(m_1, m_2)]$, and $T_4 \sim 3[\widetilde{\mathcal{D}}(m_1, m_2) + \mathcal{D}(m_1, m_2)]^2 + C_2(m_1, m_2)$, which are good in the dilute limit ($|C_1/T_1|$ and $|C_2/T_4|$ will be close to zero), we have

$$\begin{aligned}&\gamma_2(m_1, m_2) \\ &= \frac{C_1(m_1, m_2) + C_2(m_1, m_2) + 4[\widetilde{\mathcal{D}}(m_1, m_2) + \mathcal{D}(m_1, m_2)]}{\{\widetilde{\mathcal{D}}(m_1, m_2) + \mathcal{D}(m_1, m_2) + \mathcal{X}(m_1, m_2)\}^2}.\end{aligned} \tag{B11}$$

Note that C_1 and $\mathcal{X}$ depend only on τ. Similarly, C_2 and ($\widetilde{\mathcal{D}}$, $\mathcal{D}$) depend only on α. The ($\widetilde{\mathcal{D}} + \mathcal{D}$) term in the numerator will contribute to $\gamma_2(m_1, m_2)$ when $\tau = 0$ and α is very small. The approximation $T_2 = T_3 \sim \mathcal{X}(\widetilde{\mathcal{D}} + \mathcal{D})$ is crucial in obtaining the numerator in Eq. (B11) with no cross terms involving the α and τ parameters. With this, we have k_4 to be the sum of k_4's coming from $X(2)$ and $D(2)$ matrices [note that, as mentioned before, $X(2) = A \oplus B \oplus C$ and $D(2) = D + \widetilde{D}$].

To test the accuracy of the formulas for M_r given by Eqs. (B1)–(B6), the binary correlation results for $\gamma_1(m, \pm)$ and $\gamma_2(m, \pm)$ are compared with exact results obtained using the eigenvalues from EGOE(1 + 2)-π ensembles with 100 members for several values of (N_+, N_-, m) and (τ, α) parameters in Table III. Extension of Eq. (11) along with the results derived for $M_r(m_1, m_2)$ will give the binary correlation results for $\gamma_1(m, \pm)$ and $\gamma_2(m, \pm)$. It is clearly seen from the results in the table that, in all the examples considered, the binary correlation results are quite close to the exact results. Similar agreements are also seen in many other examples which are not shown in thetable.

[1] C. E. Porter, *Statistical Theories of Spectra: Fluctuations* (Academic, New York, 1965).
[2] M. L. Mehta, *Random Matrices*, 3rd ed. (Elsevier, Amsterdam, 2004).
[3] T. A. Brody, J. Flores, J. B. French, P. A. Mello, A. Pandey, and S. S. M. Wong, Rev. Mod. Phys. **53**, 385 (1981).
[4] R. U. Haq, A. Pandey, and O. Bohigas, Phys. Rev. Lett. **48**, 1086 (1982).
[5] V. Zelevinsky, B. A. Brown, N. Frazier, and M. Horoi, Phys. Rep. **276**, 85 (1996).
[6] T. Guhr, A. Müller-Groeling, and H. A. Weidenmüller, Phys. Rep. **299**, 189 (1998).
[7] D. Ullmo, Rep. Prog. Phys. **71**, 026001 (2008).
[8] F. Haake, *Quantum Signatures of Chaos* (Springer, New York, 2010).
[9] J. M. G. Gómez, K. Kar, V. K. B. Kota, R. A. Molina, A. Relaño, and J. Retamosa, Phys. Rep. **499**, 103 (2011).
[10] H. A. Weidenmüller and G. E. Mitchell, Rev. Mod. Phys. **81**, 539 (2009).
[11] G. E. Mitchell, A. Richter, and H. A. Weidenmüller, Rev. Mod. Phys. **82**, 2845 (2010).
[12] J. B. French and S. S. M. Wong, Phys. Lett. B **33**, 449 (1970).
[13] O. Bohigas and J. Flores, Phys. Lett. B **34**, 261 (1971).
[14] V. K. B. Kota, Phys. Rep. **347**, 223 (2001).
[15] V. K. B. Kota and R. U. Haq, *Spectral Distributions in Nuclei and Statistical Spectroscopy* (World Scientific, Singapore, 2010).
[16] Ph. Jacquod and A. D. Stone, Phys. Rev. B **64**, 214416 (2001).
[17] T. Papenbrock, L. Kaplan, and G. F. Bertsch, Phys. Rev. B **65**, 235120 (2002).
[18] Manan Vyas, V. K. B. Kota, and N. D. Chavda, Phys. Rev. E **81**, 036212 (2010).

[19] Manan Vyas, V. K. B. Kota, and N. D. Chavda, Phys. Lett. A **373**, 1434 (2009).
[20] Manan Vyas, N. D. Chavda, V. K. B. Kota, and V. Potbhare, arXiv:1010.6054.
[21] Manan Vyas and V. K. B. Kota, Ann. Phys. (NY) **325**, 2451 (2010).
[22] T. Papenbrock and H. A. Weidenmüller, Rev. Mod. Phys. **79**, 997 (2007).
[23] Y. Alhassid, H. A. Weidenmüller, and A. Wobst, Phys. Rev. B **72**, 045318 (2005).
[24] D. Kusnezov, Phys. Rev. Lett. **85**, 3773 (2000).
[25] D. Mocelj, T. Rauscher, G. Martínez-Pinedo, K. Langanke, L. Pacearescu, A. Faessler, F.-K. Thielemann, and Y. Alhassid, Phys. Rev. C **75**, 045805 (2007).
[26] V. Zelevinsky and A. Volya, Phys. Rep. **391**, 311 (2004).
[27] Y. M. Zhao, A. Arima, and N. Yoshinaga, Phys. Rep. **400**, 1 (2004).
[28] Y. M. Zhao, A. Arima, N. Shimizu, K. Ogawa, N. Yoshinaga, and O. Scholten, Phys. Rev. C **70**, 054322 (2004).
[29] T. Papenbrock and H. A. Weidenmüller, Phys. Rev. C **78**, 054305 (2008).
[30] F. S. Chang, J. B. French, and T. H. Thio, Ann. Phys. (NY) **66**, 137 (1971).
[31] K. K. Mon, B. A. dissertation, Princeton University, 1973.
[32] K. K. Mon and J. B. French, Ann. Phys. (NY) **95**, 90 (1975).
[33] S. Tomsovic, Ph.D. thesis, University of Rochester, 1986.
[34] J. B. French, V. K. B. Kota, A. Pandey, and S. Tomsovic, Ann. Phys. (NY) **181**, 235 (1988).
[35] J. B. French and K. F. Ratcliff, Phys. Rev. C **3**, 94 (1971).
[36] S. S. M. Wong, *Nuclear Statistical Spectroscopy* (Oxford University Press, New York, 1986).
[37] M. Nomura, Prog. Theor. Phys. **48**, 110 (1972).
[38] S. Ayik and J. N. Ginocchio, Nucl. Phys. A **221**, 285 (1974).
[39] V. Potbhare, Ph.D. thesis, University of Rochester, 1975.
[40] B. D. Chang and S. S. M. Wong, Nucl. Phys. A **294**, 19 (1978).
[41] J. Karwowski, F. Rajadell, J. Planelles, and V. Mas, At. Data Nucl. Data Tables **61**, 177 (1995).
[42] J. Planelles, F. Rajadell, and J. Karwowski, J. Phys. A: Math. Gen. **30**, 2181 (1997).
[43] E. Terán and C. W. Johnson, Phys. Rev. C **73**, 024303 (2006).
[44] Manan Vyas, Ph.D. thesis, submitted to M. S. University of Baroda, India, 2011.
[45] V. K. B. Kota, D. Majumdar, R. Haq, and R. J. Leclair, Can. J. Phys. **77**, 893 (1999).
[46] F. Nowacki and A. Poves, Phys. Rev. C **79**, 014310 (2009).
[47] O. Sorlin *et al.*, Phys. Rev. Lett. **88**, 092501 (2002).
[48] S. M. Grimes and T. N. Massey, Phys. Rev. C **51**, 606 (1995).
[49] E. Terán and C. W. Johnson, Phys. Rev. C **74**, 067302 (2006).
[50] A. Stuart and J. K. Ord, *Kendall's Advanced Theory of Statistics: Distribution Theory* (Oxford University Press, New York, 1987).